



Contents lists available at SciVerse ScienceDirect

China University of Geosciences (Beijing)



Geoscience Frontiers

journal homepage: www.elsevier.com/locate/gsf

Research paper

Periodicities in the emplacement of large igneous provinces through the Phanerozoic: Relations to ocean chemistry and marine biodiversity evolution

Andreas Prokoph ^{a,*}, Hafida El Bilali ^b, Richard Ernst ^{b,c}^a Speedstat, 19 Langstrom Crescent, Ottawa, ON K1G 5J5, Canada^b Carleton University, Department of Earth Sciences, Herzberg Building, Ottawa, ON K1S 5B6, Canada^c ErnstGeosciences, 43 Margrave Avenue, Ottawa, ON K1T 3Y2, Canada

ARTICLE INFO

Article history:

Received 21 April 2012

Received in revised form

20 July 2012

Accepted 10 August 2012

Available online 25 August 2012

Keywords:

Large igneous provinces

Wavelet transform

Sulfur isotope

Mantle plume

Marine biodiversity

Periodicity

ABSTRACT

Large igneous provinces (LIPs) are considered a relevant cause for mass extinctions of marine life throughout Earth's history. Their flood basalts and associated intrusions can cause significant release of SO_4 and CO_2 and consequently, cause major environmental disruptions. Here, we reconstruct the long-term periodic pattern of LIP emplacement and its impact on ocean chemistry and biodiversity from $\delta^{34}\text{S}_{\text{sulfate}}$ of the last 520 Ma under particular consideration of the preservation limits of LIP records. A combination of cross-wavelet and other time-series analysis methods has been applied to quantify a potential chain of linkage between LIP emplacement periodicity, geochemical changes and the Phanerozoic marine genera record. We suggest a mantle plume cyclicity represented by LIP volumes (V) of $V = -(350-770) \times 10^3 \text{ km}^3 \sin(2\pi t/170 \text{ Ma}) + (300-650) \times 10^3 \text{ km}^3 \sin(2\pi t/64.5 \text{ Ma} + 2.3)$ for t = time in Ma. A shift from the 64.5 Ma to a weaker ~28–35 Ma LIP cyclicity during the Jurassic contributes together with probably independent changes in the marine sulfur cycle to less ocean anoxia, and a general stabilization of ocean chemistry and increasing marine biodiversity throughout the last ~135 Ma. The LIP cycle pattern is coherent with marine biodiversity fluctuations corresponding to a reduction of marine biodiversity of ~120 genera/Ma at $\sim 600 \times 10^3 \text{ km}^3$ LIP eruption volume. The 62–65 Ma LIP cycle pattern as well as excursion in $\delta^{34}\text{S}_{\text{sulfate}}$ and marine genera reduction suggest a not-yet identified found LIP event at ~440–450 Ma.

© 2013, China University of Geosciences (Beijing) and Peking University. Production and hosting by Elsevier B.V. All rights reserved.

1. Introduction

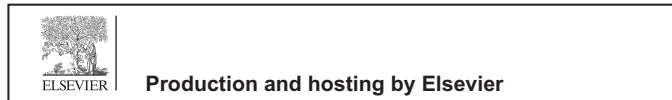
Flood basalts and their associated plumbing systems represent large igneous provinces (LIPs) and are typically linked to mantle plumes that originate from deep in the mantle (e.g., Coffin and Eldholm, 1994; Ernst and Buchan, 2001; Courtillot et al., 2003) triggering large volume gas release in the ocean-atmospheric systems. Numerous studies have attempted to explore the links

between the type, duration and magnitude of specific LIPs and temporally associated environmental perturbations (e.g., Caldeira and Rampino, 1993; Wignall, 2001; Berner, 2002; Svensen et al., 2009). In addition, there have also been evaluations of a long-term statistical link between the cycle of LIPs, ocean chemistry and biodiversity over the last 230 Ma and purely based on coeval timing of events (e.g., Caldeira and Rampino, 1993). A timing link between LIPs and mass extinctions has been discussed for several decades (e.g., Wignall, 2001; Courtillot and Renne, 2003), with ongoing high-resolution studies complementing this relationship (e.g., Isozaki, 2009; Saunders and Reichow, 2009). A recently discovered ~62 Ma and ~140 Ma cyclicity in the complete Phanerozoic marine fossil record (Rhode and Muller, 2005) has re-ignited the quest for primary and secondary geological factors that might have caused these repeated fluctuations. For example, the ~62 Ma cyclicity in LIP, $^{87}\text{Sr}/^{86}\text{Sr}$ and $\delta^{34}\text{S}_{\text{sulfate}}$ records detected in independent studies (Prokoph et al., 2004a, 2008) have been merged to explain such patterns and possible relationships between these cycles (Melott et al., 2012).

* Corresponding author.

E-mail addresses: aprokocon@aol.com (A. Prokoph), [\(H. El Bilali\)](mailto:elbilalihaf@hotmail.com), Richard.Ernst@ErnstGeosciences.com (R. Ernst).

Peer-review under responsibility of China University of Geosciences (Beijing).



Production and hosting by Elsevier

Here we attempt to reconstruct potential links between large-scale magmatism, ocean chemistry and biological evolution based on new databases and, for the first time, using cross-wavelet analysis to trace the cycles and their coherency through time and detect abrupt and gradual change. We used marine isotope records of sulfur and strontium as potentially continuous proxies for variability of igneous magmatism, in particular mantle plume related LIP eruptions. Moreover we used LIP volumes to better quantify magnitude relationships between LIP, oceanic chemistry and marine biodiversity evolution. The main challenging feature of the LIP record is its incompleteness. The LIP database is frequently updated with new LIPs being recognized as well as improvements in the ages, areal and volume extent of known LIPs (e.g., Torsvik et al., 2008; Reichow et al., 2009; Bryan et al., 2010; Ernst and Bleeker, 2010). However, the best dated and defined group of LIPs called “A10” (Ernst and Buchan, 2001) through the last 520 Ma have not changed or amended except for an increase in the ages of some LIPs dated only by the Ar/Ar method. The astronomical cycle based calibration of Fish Canyon sanidine reduced the $^{40}\text{Ar}/^{39}\text{Ar}$ method’s absolute uncertainty from $\sim 2.5\%$ to 0.25% , and more importantly increased the absolute age of $^{40}\text{Ar}/^{39}\text{Ar}$ -based dates by $\sim 0.6\%$ (Kuiper et al., 2008). In this way, the age-determination issues around the Permian–Triassic boundary are an exception. Considering the age uncertainties mentioned above and the biostratigraphic resolution to which fossil and geochemical records are fitted (e.g., Prokoph et al., 2008) the LIP records can be used for statistical robust comparison with other long-term geological records at ± 2 Ma resolution. However, the A10-record does not include information on the size of the LIP, thus cannot provide a link between the magnitudes of an LIP and environmental changes.

2. Datasets and their compilation

For our study, we used updated databases of probability-weighted LIP initiation ages and volumes (Ernst and Buchan, 2001; Courtillot and Renne, 2003), $\delta^{34}\text{S}_{\text{sulfate}}$ (Kampschulte and Strauss, 2004; Paytan et al., 2004) and $^{87}\text{Sr}/^{86}\text{Sr}$ (Prokoph et al., 2008), and marine biodiversity (Sepkoski, 2002; Rhode and Muller, 2005) for the last 520 Ma with reference to the GTS2004 time scale (Gradstein et al., 2005). The LIP volume dataset has two versions. Version #1 uses the minimal value for volume ranges and also reduces the estimated oceanic LIP volumes by 50% to remove the amount that is associated with underplating. This results in a better comparison with continental LIPs where the component of underplating is typically not possible to estimate. The version #2 estimate of LIP volumes consists of the maximum LIP volumes including the underplate component for oceanic LIPs. Both LIP volume datasets are restricted to the last 260 Ma due to the availability of reliable volume data.

Each dataset has been Gaussian filtered to equidistant 1 Ma-intervals considering a minimum 2% stratigraphic uncertainty (95% confidence interval of normal distribution). The Gaussian filtering algorithm used is in detail described in Prokoph et al. (2004a). The mean sample age uncertainty is set larger for poorly stratigraphic constraint samples. The Gaussian filtered records for LIP occurrences and volumes are shown in Fig. 1.

3. Data analysis methods

Continuous wavelet transform (CWT) is applied to delineate temporal variations of cycle amplitudes and phase over a 20–500 Ma spectrum for all datasets, whereas cross-wavelet transform (XWT) is used to extract the cross-amplitude and instantaneous time lag (i.e. phase shift) between LIP and other geological records.

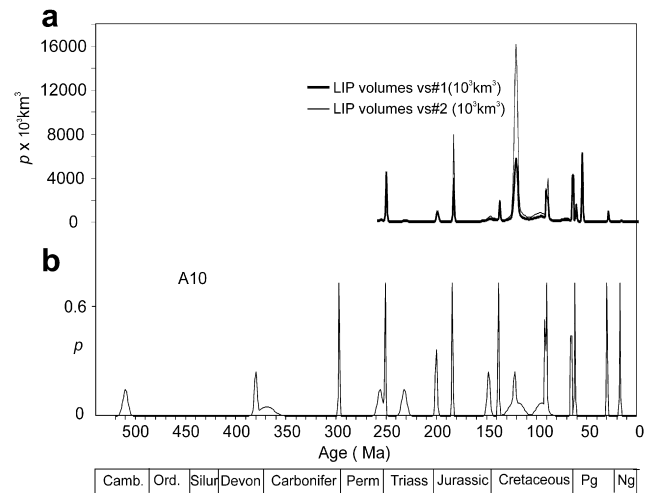


Figure 1. Gaussian filtered LIP volumes for last 260 Ma and A10 occurrences for last 520 Ma. For raw data see Ernst and Buchan (2001) and Table 1, for Gaussian filtered data see Table 2.

Wavelet analysis first emerged as a filtering and data compression method in the 1980s (e.g., Morlet et al., 1982). Wavelet analysis transforms a time-series into a frequency domain; it simultaneously transforms the ‘depth’ or ‘time’ domain and the ‘scale’ or ‘frequency’ domain by using various shapes and sizes of short filtering functions called wavelets. CWT allows for the

Table 1
LIP volumes.

| Age (Ma) | 1σ | Rating | Vol-vs.#1 (10^3 km^3) | Vol-vs.#2 (10^3 km^3) | Type | Event ID | Event name |
|-------------|-----------|--------|--------------------------------------|--------------------------------------|-------------|-------------|---|
| 17 | 0.5 | A | 175 | 175 | Continental | 1 | Columbia |
| 30 | 0.5 | A | 1200* | 1200* | Continental | 2 | Afar |
| 48 | 5 | B | 50\$ | 100\$ | Oceanic | – | Metchosin ("Coast Range Basalt Province") |
| 56* | 0.5 | A | 7900* | 7900* | Continental | 5 | NAVP |
| 62 | 0.5 | A | 2000* | 2000* | Continental | 5 | NAVP |
| 65.5 | 0.5 | A | 8600 | 8600 | Continental | 6 | Deccan |
| 70 | 1 | B | 100\$ | 200\$ | Oceanic | 9 | Carmacks |
| 73 | 5 | B | 600 | 1200 | Oceanic | 7 | Maud |
| 73 | 5 | B | 1250 | 2500 | Oceanic | 8 | Sierra |
| 90 | 0.5 | A | 2250 | 4500 | Oceanic | 11 | CCIP |
| 91.6 | 0.5 | A | 4400 | 4400 | Continental | 10 | Madagascar |
| 95 | 5 | A | 2000\$ | 2000\$ | Continental | 12 | Alpha |
| 96 | 5 | B | 750 | 1500 | Oceanic | 13 | Wallaby |
| 99 | 7.5 | B | 4550 | 9100 | Oceanic | 14 | Hess |
| 101 | 5 | B | 600 | 1200 | Oceanic | 15 | Naturaliste |
| 111 | 5 | B | 450 | 900 | Oceanic | 19 | Nauru |
| 118 | 5 | A | 3000* | 6000* | Oceanic | 18 | Kerguelen |
| 122 | 1.5 | A | 20,000# | 57,000# | Oceanic | 20 | Ontong |
| 123 | 5 | A | 4400 | 8800 | Oceanic | 21 | Manihiki |
| 123 | 6.5 | B | 50\$ | 100\$ | Oceanic | 22 | Piñón |
| 136 | 5 | B | 800 | 800 | Continental | 25 | Gascoyne |
| 138 | 0.5 | A | 2300 | 2300 | Continental | 24 | Paraná–Etendeka |
| 145 | 5 | B | 900 | 1800 | Oceanic | 26 | Magellan |
| 147 | 5 | B | 1250 | 2500 | Oceanic | 27 | Shatsky |
| 148 | 1.5 | A | 300 | 600 | Oceanic | 28 | Sorachi |
| 155 | 5 | B | 300\$ | 300\$ | Continental | 29 | Argo |
| 184 | 0.5 | A | 5000# | 10,000# | Continental | 31 | Karoo–Ferrar |
| 200 | 1 | A | 2500 | 2500 | Continental | 32 | CAMP |
| 214 | 7 | B | 225\$ | 450\$ | Oceanic | 33 | Angayucham ("Ramparts Group volcanics") |
| 232 | 2.5 | A | 500 | 1000 | Oceanic | 34 | Wrangelia |
| 251 | 0.5 | A | 5700 | 5700 | Continental | 36 | Siberian |
| 256 | 2.5 | A | 1000 | 1000 | Continental | 37 | Emeishan |

Estimation by Ernst and Buchan (2001) except for * Courtillot and Renne (2003), \$ estimates from areal extend, # volume estimates from 5000 to $10,000 \times 10^3 \text{ km}^3$.

Table 2
Gaussian filtered data.

| Age (Ma) | A10 <i>p</i> | $^{87}\text{Sr}/^{86}\text{Sr}$ | $\delta^{34}\text{S}$ | LIP volumes vs#1(10^3 km^3) | LIP volumes vs#2(10^3 km^3) | Marine genera* | Age (Ma) | A10 <i>p</i> | $^{87}\text{Sr}/^{86}\text{Sr}$ | $\delta^{34}\text{S}$ | LIP volumes vs#1(10^3 km^3) | LIP volumes vs#2(10^3 km^3) | Marine genera* |
|---------------|-----------------|---------------------------------|-----------------------|--|--|-------------------|----------|-----------------|---------------------------------|-----------------------|--|--|-------------------|
| Part-1 | | | | | | | | | | | | | |
| 0 | 0 | 0.709167 | 21.1264 | 0.0 | 0.0 | 189.7 | 71 | 0 | 0.707713 | 19.2839 | 160.7 | 321.4 | 84.3 |
| 1 | 0 | 0.709134 | 21.8869 | 0.0 | 0.0 | 227.3 | 72 | 0 | 0.707693 | 19.2951 | 150.5 | 300.9 | 105.2 |
| 2 | 0 | 0.70908 | 22.0149 | 0.0 | 0.0 | 161.1 | 73 | 0 | 0.707696 | 19.2447 | 148.7 | 297.3 | 125.8 |
| 3 | 0 | 0.709055 | 21.5815 | 0.0 | 0.0 | 198.2 | 74 | 0.00001 | 0.707624 | 19.1532 | 145.7 | 291.3 | 146.3 |
| 4 | 0 | 0.709042 | 21.596 | 0.0 | 0.0 | 114 | 75 | 0.00003 | 0.707618 | 19.044 | 137.8 | 275.5 | 166.5 |
| 5 | 0 | 0.709001 | 21.9447 | 0.0 | 0.0 | 150.5 | 76 | 0.00006 | 0.707584 | 19.0431 | 125.6 | 251.1 | 186.5 |
| 6 | 0 | 0.708958 | 21.9649 | 0.0 | 0.0 | -13.7 | 77 | 0.00012 | 0.707518 | 19.0583 | 110.8 | 221.3 | 206.4 |
| 7 | 0 | 0.708949 | 22.32 | 0.0 | 0.0 | 22.3 | 78 | 0.00025 | 0.70746 | 18.9057 | 94.9 | 189.3 | 110 |
| 8 | 0 | 0.708937 | 22.0065 | 0.0 | 0.0 | 20 | 79 | 0.00048 | 0.707662 | 18.9278 | 79.9 | 158.9 | 129.4 |
| 9 | 0 | 0.708952 | 22.0175 | 0.0 | 0.0 | 55.5 | 80 | 0.00089 | 0.707542 | 18.6342 | 67.3 | 132.9 | 148.7 |
| 10 | 0 | 0.708921 | 21.9316 | 0.0 | 0.0 | 90.7 | 81 | 0.00158 | 0.707497 | 18.2425 | 58.5 | 113.8 | 167.7 |
| 11 | 0 | 0.708902 | 22.2279 | 0.0 | 0.0 | 125.7 | 82 | 0.00272 | 0.707464 | 18.1086 | 54.4 | 103.4 | 186.6 |
| 12 | 0 | 0.708857 | 22.4396 | 0.0 | 0.0 | 183.4 | 83 | 0.00448 | 0.707483 | 18.3081 | 55.9 | 102.9 | 205.2 |
| 13 | 0 | 0.70882 | 22.0326 | 0.0 | 0.0 | 217.9 | 84 | 0.00709 | 0.707474 | 18.2123 | 63.6 | 113.0 | 49.2 |
| 14 | 0 | 0.708795 | 21.9688 | 0.0 | 0.0 | 252.1 | 85 | 0.0108 | 0.70746 | 17.2443 | 77.9 | 134.2 | 5.4 |
| 15 | 0.00027 | 0.708771 | 21.8751 | 0.0 | 0.0 | 286 | 86 | 0.01579 | 0.707379 | 18.1425 | 99.1 | 166.7 | -46.5 |
| 16 | 0.10798 | 0.708743 | 22.09 | 18.9 | 18.9 | 91.7 | 87 | 0.02218 | 0.707357 | 18.2658 | 127.4 | 210.4 | -28.7 |
| 17 | 0.79789 | 0.70865 | 21.9 | 139.6 | 139.6 | 125.1 | 88 | 0.02995 | 0.707341 | 18.1779 | 163.0 | 266.0 | -60.5 |
| 18 | 0.10798 | 0.708533 | 21.8 | 18.9 | 18.9 | 158.3 | 89 | 0.10798 | 0.707317 | 18.2011 | 446.2 | 814.7 | -43 |
| 19 | 0.00027 | 0.708458 | 21.56 | 0.0 | 0.0 | 191.3 | 90 | 0.79789 | 0.707292 | 18.3897 | 2064.7 | 4011.6 | -47.7 |
| 20 | 0 | 0.708372 | 22.0059 | 0.0 | 0.0 | 223.9 | 91 | 0.38837 | 0.707318 | 18.6175 | 2247.7 | 2670.7 | -30.6 |
| 21 | 0 | 0.708347 | 22 | 0.0 | 0.0 | -1.6 | 92 | 0.57938 | 0.707399 | 18.8501 | 2892.8 | 3103.0 | -61.7 |
| 22 | 0 | 0.708313 | 21.9001 | 0.0 | 0.0 | 30.6 | 93 | 0.07365 | 0.70738 | 18.9664 | 456.1 | 695.3 | -44.9 |
| 23 | 0 | 0.708254 | 21.8988 | 0.0 | 0.0 | 62.5 | 94 | 0.07821 | 0.707408 | 19.0058 | 423.6 | 690.7 | -11.6 |
| 24 | 0 | 0.708236 | 21.6795 | 0.0 | 0.0 | -90.8 | 95 | 0.07979 | 0.707481 | 19.058 | 451.7 | 743.8 | 4.8 |
| 25 | 0 | 0.708167 | 21.7 | 0.0 | 0.0 | -59.4 | 96 | 0.07821 | 0.707463 | 19.0421 | 469.1 | 781.8 | -38.4 |
| 26 | 0 | 0.708113 | 21.7 | 0.0 | 0.0 | -28.2 | 97 | 0.07365 | 0.707459 | 18.9066 | 475.0 | 802.8 | -22.4 |
| 27 | 0 | 0.708073 | 21.3231 | 0.0 | 0.0 | 2.8 | 98 | 0.06664 | 0.707462 | 18.5743 | 469.7 | 806.1 | -31.8 |
| 28 | 0.00027 | 0.708018 | 21.3187 | 0.3 | 0.3 | 33.5 | 99 | 0.05794 | 0.707438 | 17.7801 | 454.3 | 792.7 | -16.2 |
| 29 | 0.10798 | 0.707986 | 21.3221 | 129.6 | 129.6 | -122.1 | 100 | 0.04839 | 0.707453 | 17.1615 | 430.6 | 764.5 | -67.5 |
| 30 | 0.79789 | 0.707974 | 21.4021 | 957.5 | 957.5 | -91.8 | 101 | 0.03884 | 0.707439 | 16.744 | 401.0 | 724.4 | -52.2 |
| 31 | 0.10798 | 0.707932 | 21.5722 | 129.6 | 129.6 | -61.8 | 102 | 0.02995 | 0.707451 | 16.3886 | 368.0 | 676.0 | -37.1 |
| 32 | 0.00027 | 0.707889 | 21.7698 | 0.3 | 0.4 | -32.1 | 103 | 0.02218 | 0.707451 | 15.7108 | 333.7 | 623.1 | -22.2 |
| 33 | 0 | 0.707855 | 21.6497 | 0.0 | 0.1 | -2.6 | 104 | 0.01579 | 0.707445 | 15.6043 | 300.5 | 569.5 | -97.8 |
| 34 | 0 | 0.707834 | 21.9439 | 0.1 | 0.2 | 124.7 | 105 | 0.0108 | 0.707432 | 15.3327 | 270.2 | 518.8 | -83.2 |
| 35 | 0 | 0.707817 | 22.2687 | 0.1 | 0.3 | 153.7 | 106 | 0.00709 | 0.707434 | 15.0616 | 244.3 | 474.4 | -68.9 |
| 36 | 0 | 0.707733 | 22.1497 | 0.2 | 0.4 | 182.5 | 107 | 0.00709 | 0.707415 | 14.8971 | 224.2 | 439.5 | -54.7 |
| 37 | 0 | 0.707761 | 22.3 | 0.4 | 0.7 | 211 | 108 | 0.0108 | 0.707403 | 15.6472 | 211.1 | 416.7 | -78 |
| 38 | 0 | 0.70775 | 22.5641 | 0.5 | 1.1 | 19.9 | 109 | 0.01579 | 0.707392 | 15.9739 | 205.8 | 408.4 | -64.2 |
| 39 | 0 | 0.707782 | 22.4314 | 0.8 | 1.6 | 48 | 110 | 0.02218 | 0.707368 | 16.0672 | 209.1 | 416.4 | -50.5 |
| 40 | 0 | 0.707782 | 22.1558 | 1.1 | 2.2 | 75.8 | 111 | 0.02995 | 0.707334 | 16.1565 | 221.4 | 441.8 | -37 |
| 41 | 0 | 0.707696 | 22.389 | 1.5 | 3.0 | -72.6 | 112 | 0.03884 | 0.707263 | 16.1406 | 242.6 | 484.8 | -56.4 |
| 42 | 0 | 0.707781 | 22.4 | 1.9 | 3.9 | -45.2 | 113 | 0.04839 | 0.707261 | 15.9708 | 272.3 | 544.3 | -43.3 |
| 43 | 0 | 0.707794 | 22.4 | 2.4 | 4.8 | -18 | 114 | 0.05794 | 0.70724 | 15.7347 | 309.1 | 618.0 | -30.3 |
| 44 | 0 | 0.707839 | 22.4 | 2.9 | 5.8 | 8.9 | 115 | 0.06664 | 0.707234 | 15.1992 | 351.1 | 702.2 | -17.4 |
| 45 | 0 | 0.707754 | 22.0003 | 3.3 | 6.7 | 35.6 | 116 | 0.07365 | 0.707265 | 14.9063 | 397.1 | 795.8 | -4.8 |
| 46 | 0 | 0.707751 | 22 | 3.7 | 7.4 | 62.1 | 117 | 0.07821 | 0.707275 | 15.4022 | 459.5 | 936.4 | 7.7 |
| 47 | 0 | 0.707798 | 22 | 3.9 | 7.8 | 88.3 | 118 | 0.07979 | 0.70732 | 15.5516 | 630.0 | 1389.1 | 20 |
| 48 | 0 | 0.707769 | 21.9993 | 4.0 | 8.0 | 114.3 | 119 | 0.07821 | 0.70738 | 15.2505 | 1229.1 | 3070.0 | 8.7 |
| 49 | 0 | 0.707764 | 20.6902 | 3.9 | 7.8 | -169.4 | 120 | 0.10934 | 0.707391 | 15.0415 | 2716.1 | 7290.6 | 20.7 |
| 50 | 0 | 0.707742 | 19.8639 | 3.7 | 7.4 | -143.8 | 121 | 0.21297 | 0.707396 | 16.6952 | 4795.1 | 13209.9 | 32.6 |
| 51 | 0 | 0.707705 | 18.4802 | 3.3 | 6.7 | -118.4 | 122 | 0.26596 | 0.707412 | 17.3857 | 5846.9 | 16213.8 | 44.2 |
| 52 | 0 | 0.707746 | 18.03 | 2.9 | 5.8 | -93.3 | 123 | 0.21297 | 0.707408 | 17.0443 | 4764.3 | 13146.8 | 55.7 |
| 53 | 0 | 0.707759 | 17.9558 | 2.5 | 4.9 | -68.4 | 124 | 0.10934 | 0.707349 | 17.2866 | 2656.2 | 7167.6 | 67.1 |
| 54 | 0 | 0.707753 | 17.7443 | 4.2 | 6.2 | -43.7 | 125 | 0.07365 | 0.707343 | 17.0231 | 1143.7 | 2893.7 | 2.8 |
| 55 | 0 | 0.70776 | 17.739 | 854.8 | 856.5 | -19.3 | 126 | 0.06664 | 0.70746 | 17.1023 | 524.0 | 1168.5 | 13.8 |
| 56 | 0 | 0.707753 | 17.3317 | 6304.9 | 6306.4 | -516 | 127 | 0.05794 | 0.70748 | 18.6474 | 338.6 | 682.1 | 24.7 |
| 57 | 0 | 0.707748 | 17.7957 | 854.7 | 856.4 | -492 | 128 | 0.04839 | 0.707482 | 17.895 | 267.7 | 519.1 | 4.4 |
| 58 | 0 | 0.707773 | 17.5923 | 4.3 | 6.5 | -581.7 | 129 | 0.03884 | 0.70747 | 17.5778 | 218.9 | 414.0 | 15 |
| 59 | 0 | 0.707749 | 18.154 | 3.3 | 6.6 | -558.1 | 130 | 0.02995 | 0.707464 | 16.9537 | 179.2 | 327.3 | -14.1 |
| 60 | 0.00027 | 0.707807 | 18.1501 | 5.8 | 11.0 | -534.8 | 131 | 0.02218 | 0.707473 | 17.0843 | 148.0 | 257.2 | -3.8 |
| 61 | 0.10798 | 0.707814 | 18.15 | 224.4 | 232.8 | -693.1 | 132 | 0.01579 | 0.707441 | 17.6692 | 125.3 | 204.3 | 6.27 |
| 62 | 0.79789 | 0.707775 | 18.7608 | 1609.0 | 1622.2 | -670.2 | 133 | 0.0108 | 0.70742 | 16.38 | 110.4 | 167.6 | 16.22 |
| 63 | 0.10798 | 0.707821 | 18.9709 | 236.0 | 256.0 | -728.9 | 134 | 0.00709 | 0.707406 | 16.3242 | 102.1 | 145.3 | 11.01 |
| 64 | 0.00886 | 0.707833 | 18.9803 | 106.0 | 135.2 | -706.4 | 135 | 0.00448 | 0.707394 | 17.4607 | 98.9 | 135.2 | 20.66 |
| 65 | 0.48394 | 0.707862 | 18.9033 | 4203.0 | 4244.0 | -684.1 | 136 | 0.00272 | 0.707385 | 17.4502 | 100.3 | 136.1 | 30.16 |
| 66 | 0.48394 | 0.707836 | 17.4117 | 4217.3 | 4272.8 | -243.5 | 137 | 0.10798 | 0.707365 | 17.3745 | 351.9 | 392.8 | 24 |
| 67 | 0.00886 | 0.707791 | 18.8377 | 148.5 | 220.9 | -221.6 | 138 | 0.79789 | 0.707349 | 18.257 | 1945.0 | 1995.9 | 33.2 |
| 68 | 0 | 0.707785 | 18.9015 | 95.0 | 190.0 | -199.9 | 139 | 0.10798 | 0.707319 | 18.3654 | 366.8 | 431.7 | 9.75 |
| 69 | 0 | 0.707759 | 19.1312 | 131.5 | 262.9 | 51.5 | 140 | 0.00027 | 0.707259 | 15.4784 | 129.4 | 211.6 | 18.66 |
| 70 | 0 | 0.707727 | 19.2274 | 163.3 | 326.7 | 72.8 | 141 | 0.00012 | 0.707263 | 13.1158 | 140.5 | 241.8 | -6.58 |

(Continued on next page)

Table 2 (Continued)

| Age (Ma) | A10 <i>p</i> | $^{87}\text{Sr}/^{86}\text{Sr}$ | $\delta^{34}\text{S}$ | LIP volumes vs#1(10^3 km^3) | LIP volumes vs#2(10^3 km^3) | Marine genera* | Age (Ma) | A10 <i>p</i> | $^{87}\text{Sr}/^{86}\text{Sr}$ | $\delta^{34}\text{S}$ | LIP volumes vs#1(10^3 km^3) | LIP volumes vs#2(10^3 km^3) | Marine genera* |
|---------------|-----------------|---------------------------------|-----------------------|--|--|-------------------|----------|-----------------|---------------------------------|-----------------------|--|--|-------------------|
| Part-2 | | | | | | | | | | | | | |
| 142 | 0.00009 | 0.707276 | 13.0023 | 152.7 | 273.5 | 2.03 | 212 | 0 | 0.707749 | 18.9209 | 12.3 | 24.6 | -7.84 |
| 143 | 0.00103 | 0.707324 | 13.0001 | 164.5 | 303.6 | -3.5 | 213 | 0 | 0.707734 | 18.9512 | 12.7 | 25.4 | 12.02 |
| 144 | 0.0076 | 0.707321 | 13 | 175.9 | 332.0 | 4.83 | 214 | 0 | 0.707715 | 18.9514 | 12.8 | 25.6 | 12.48 |
| 145 | 0.03599 | 0.707299 | 13 | 190.6 | 365.3 | 13.01 | 215 | 0 | 0.707704 | 18.8113 | 12.7 | 25.4 | 12.85 |
| 146 | 0.10934 | 0.707231 | 13.0001 | 214.3 | 415.3 | 124.06 | 216 | 0 | 0.707705 | 18.7543 | 12.3 | 24.6 | 13.14 |
| 147 | 0.21297 | 0.707188 | 13.0377 | 242.3 | 472.2 | 131.96 | 217 | 0 | 0.707703 | 18.8801 | 11.7 | 23.4 | 26.85 |
| 148 | 0.26596 | 0.707163 | 16.0002 | 250.1 | 487.6 | 139.72 | 218 | 0 | 0.707696 | 19.0565 | 10.9 | 21.8 | 26.98 |
| 149 | 0.21297 | 0.707109 | 16 | 221.9 | 430.0 | 161.85 | 219 | 0 | 0.707684 | 19.2308 | 9.9 | 19.9 | 27.04 |
| 150 | 0.10934 | 0.707024 | 16 | 175.4 | 335.1 | 169.33 | 220 | 0 | 0.707671 | 19.3747 | 8.9 | 17.8 | 27.01 |
| 151 | 0.03599 | 0.706985 | 16 | 136.3 | 254.4 | 189.68 | 221 | 0.00001 | 0.707666 | 19.4817 | 7.8 | 15.6 | 26.91 |
| 152 | 0.0076 | 0.706931 | 16 | 110.1 | 199.8 | 196.89 | 222 | 0.00005 | 0.707669 | 19.5474 | 6.7 | 13.4 | 26.74 |
| 153 | 0.00103 | 0.706874 | 16 | 91.1 | 159.9 | 203.97 | 223 | 0.00024 | 0.707653 | 18.046 | 5.7 | 11.5 | 19.49 |
| 154 | 0.00009 | 0.706854 | 16 | 75.2 | 126.9 | 218.41 | 224 | 0.00095 | 0.707624 | 17.9001 | 5.1 | 10.2 | 19.16 |
| 155 | 0 | 0.706847 | 16 | 61.4 | 98.9 | 225.22 | 225 | 0.00317 | 0.707606 | 17.8998 | 5.3 | 10.6 | 18.76 |
| 156 | 0 | 0.706865 | 15.9999 | 49.6 | 75.7 | 234.2 | 226 | 0.00896 | 0.707597 | 17.8986 | 7.4 | 14.9 | 18.29 |
| 157 | 0 | 0.706884 | 15.7084 | 39.6 | 57.2 | 240.74 | 227 | 0.0216 | 0.707601 | 17.8903 | 13.1 | 26.2 | 17.75 |
| 158 | 0 | 0.706886 | 15.4001 | 31.3 | 42.6 | 191.18 | 228 | 0.04437 | 0.707613 | 17.8373 | 23.9 | 47.8 | -29.86 |
| 159 | 0 | 0.706874 | 15.4006 | 24.4 | 31.4 | 197.47 | 229 | 0.07767 | 0.707636 | 17.6277 | 40.1 | 80.3 | -30.54 |
| 160 | 0 | 0.706855 | 15.4237 | 18.7 | 22.9 | 207.62 | 230 | 0.11588 | 0.707678 | 17.4056 | 58.9 | 117.8 | -31.3 |
| 161 | 0 | 0.706851 | 15.8395 | 14.1 | 16.5 | 213.65 | 231 | 0.14731 | 0.707713 | 17.5076 | 74.3 | 148.7 | -32.11 |
| 162 | 0 | 0.706856 | 16.156 | 10.3 | 11.6 | 186.88 | 232 | 0.15958 | 0.707725 | 18.2927 | 80.3 | 160.5 | -33 |
| 163 | 0 | 0.706881 | 16.1469 | 7.4 | 8.1 | 184.31 | 233 | 0.14731 | 0.707726 | 19.2869 | 74.0 | 148.0 | -119.95 |
| 164 | 0 | 0.707018 | 16.1415 | 5.1 | 5.5 | 187.63 | 234 | 0.11588 | 0.707723 | 20.5775 | 58.2 | 116.3 | -120.97 |
| 165 | 0 | 0.70712 | 16.9574 | 3.4 | 3.6 | 184.15 | 235 | 0.07767 | 0.70772 | 23.026 | 39.0 | 78.0 | -122.05 |
| 166 | 0 | 0.707106 | 18.6813 | 2.2 | 2.3 | 138.87 | 236 | 0.04437 | 0.707726 | 23.9151 | 22.3 | 44.6 | -123.2 |
| 167 | 0 | 0.707084 | 20.1853 | 1.4 | 1.4 | 125.49 | 237 | 0.0216 | 0.707746 | 23.1014 | 10.9 | 21.7 | -178.57 |
| 168 | 0 | 0.707092 | 18.9971 | 0.8 | 0.8 | 121.97 | 238 | 0.00896 | 0.707778 | 22.409 | 4.5 | 9.0 | -179.84 |
| 169 | 0 | 0.707146 | 17.2493 | 0.5 | 0.5 | 126.99 | 239 | 0.00317 | 0.707833 | 22.8929 | 1.6 | 3.2 | -181.17 |
| 170 | 0 | 0.707241 | 16.4589 | 0.3 | 0.3 | 70.4 | 240 | 0.00095 | 0.707869 | 23.2407 | 0.5 | 1.0 | -232.22 |
| 171 | 0 | 0.707282 | 17.0917 | 0.1 | 0.1 | 75.19 | 241 | 0.00024 | 0.707878 | 22.6934 | 0.1 | 0.3 | -233.67 |
| 172 | 0 | 0.707292 | 17.7408 | 0.1 | 0.1 | 12.36 | 242 | 0.00005 | 0.707891 | 21.7016 | 0.0 | 0.1 | -235.18 |
| 173 | 0 | 0.707295 | 17.9352 | 0.0 | 0.0 | 16.91 | 243 | 0.00001 | 0.707943 | 22.8395 | 0.0 | 0.0 | -291.42 |
| 174 | 0 | 0.707291 | 17.9011 | 0.0 | 0.0 | 21.34 | 244 | 0 | 0.708054 | 25.9221 | 0.0 | 0.0 | -293.04 |
| 175 | 0 | 0.70729 | 17.9 | 0.0 | 0.0 | 25.66 | 245 | 0.00001 | 0.708131 | 26.3229 | 0.0 | 0.0 | -342.72 |
| 176 | 0 | 0.707291 | 17.9009 | 0.0 | 0.0 | -36.14 | 246 | 0.00005 | 0.708152 | 26.327 | 0.1 | 0.1 | -344.45 |
| 177 | 0 | 0.707299 | 18.0826 | 0.0 | 0.0 | -32.05 | 247 | 0.00024 | 0.708123 | 25.7205 | 0.2 | 0.2 | -346.24 |
| 178 | 0 | 0.707306 | 22.7007 | 0.0 | 0.0 | -28.08 | 248 | 0.00095 | 0.707986 | 19.6957 | 1.0 | 1.0 | -393.58 |
| 179 | 0 | 0.707292 | 23.1057 | 0.0 | 0.0 | -24.22 | 249 | 0.00317 | 0.707794 | 16.6393 | 4.7 | 4.7 | -395.48 |
| 180 | 0 | 0.707248 | 22.5517 | 0.0 | 0.0 | -8.97 | 250 | 0.10798 | 0.70764 | 17.1165 | 624.5 | 624.5 | -425.42 |
| 181 | 0 | 0.707193 | 21.1139 | 0.0 | 0.0 | -5.33 | 251 | 0.79789 | 0.707513 | 17.7684 | 4569.5 | 4569.5 | -212.41 |
| 182 | 0.00027 | 0.707147 | 18.7136 | 1.3 | 2.7 | -1.81 | 252 | 0.10798 | 0.707406 | 18.3852 | 659.9 | 659.9 | -214.46 |
| 183 | 0.10798 | 0.707116 | 17.4601 | 539.9 | 1079.8 | 2.11 | 253 | 0.07767 | 0.707327 | 18.9415 | 79.2 | 79.2 | -216.55 |
| 184 | 0.79789 | 0.707134 | 17.1609 | 3989.4 | 7978.9 | 5.42 | 254 | 0.11588 | 0.707301 | 19.4297 | 115.9 | 115.9 | -66.2 |
| 185 | 0.10798 | 0.70719 | 15.7734 | 539.9 | 1079.8 | 8.62 | 255 | 0.14731 | 0.707305 | 19.8524 | 147.3 | 147.3 | -68.38 |
| 186 | 0.00027 | 0.70723 | 14.4379 | 1.3 | 2.7 | 11.71 | 256 | 0.15958 | 0.707288 | 20.217 | 159.6 | 159.6 | -70.62 |
| 187 | 0 | 0.707261 | 14.3132 | 0.0 | 0.0 | -18.8 | 257 | 0.14731 | 0.707208 | 19.6539 | 147.3 | 147.3 | -72.9 |
| 188 | 0 | 0.707298 | 14.6137 | 0.0 | 0.0 | -15.92 | 258 | 0.11588 | 0.707123 | 11.0246 | 115.9 | 115.9 | -75.22 |
| 189 | 0 | 0.707345 | 15.3098 | 0.0 | 0.0 | -13.14 | 259 | 0.07767 | 0.707096 | 11.0001 | 77.7 | 77.7 | -77.59 |
| 190 | 0 | 0.707398 | 15.1189 | 0.0 | 0.1 | -63.46 | 260 | 0.04437 | 0.707128 | 11.0006 | 44.4 | 44.4 | -80.01 |
| 191 | 0 | 0.707443 | 14.8533 | 0.1 | 0.1 | -60.89 | 261 | 0.0216 | 0.707196 | 11.0043 | | | 178.04 |
| 192 | 0 | 0.707482 | 14.6072 | 0.1 | 0.2 | -58.42 | 262 | 0.00896 | 0.707197 | 11.0298 | | | 175.55 |
| 193 | 0 | 0.707528 | 14.4269 | 0.1 | 0.3 | -56.05 | 263 | 0.03017 | 0.707096 | 11.1977 | | | 173.01 |
| 194 | 0 | 0.707583 | 14.3169 | 0.2 | 0.4 | -121.28 | 264 | 0.00095 | 0.707067 | 12.0092 | | | 170.44 |
| 195 | 0 | 0.707652 | 14.7292 | 0.3 | 0.6 | -119.11 | 265 | 0.00024 | 0.707119 | 13.4035 | | | 167.82 |
| 196 | 0.00013 | 0.707717 | 24.1911 | 0.8 | 1.3 | -117.03 | 266 | 0.00005 | 0.707184 | 13.9802 | | | 260.67 |
| 197 | 0.00443 | 0.707748 | 24.0619 | 11.8 | 12.4 | -170.56 | 267 | 0.00001 | 0.707188 | 14.0819 | | | 257.99 |
| 198 | 0.05399 | 0.707757 | 23.5983 | 135.9 | 136.9 | -168.68 | 268 | 0 | 0.70714 | 14.0837 | | | 255.26 |
| 199 | 0.24197 | 0.707759 | 22.3601 | 606.2 | 607.5 | -209.39 | 269 | 0 | 0.707102 | 13.9591 | | | 252.51 |
| 200 | 0.39894 | 0.707745 | 19.7228 | 999.1 | 1000.8 | -103.71 | 270 | 0 | 0.707085 | 13.6231 | | | 249.71 |
| 201 | 0.24197 | 0.707734 | 16.1006 | 607.2 | 609.5 | -102.11 | 271 | 0 | 0.707067 | 13.5371 | | | 280.22 |
| 202 | 0.05399 | 0.707749 | 13.5559 | 137.9 | 140.9 | -100.61 | 272 | 0 | 0.707037 | 13.7333 | | | 277.36 |
| 203 | 0.00443 | 0.707821 | 15.7744 | 14.8 | 18.5 | -99.2 | 273 | 0 | 0.707011 | 14.5791 | | | 274.47 |
| 204 | 0.00013 | 0.70799 | 17.9649 | 5.0 | 9.6 | -37.55 | 274 | 0 | 0.706997 | 15.1666 | | | 271.55 |
| 205 | 0 | 0.708046 | 18.0653 | 5.6 | 11.2 | -36.32 | 275 | 0 | 0.707006 | 15.1211 | | | 268.6 |
| 206 | 0 | 0.708043 | 18.1393 | 6.7 | 13.3 | -35.18 | 276 | 0 | 0.70706 | 14.4292 | | | 229.29 |
| 207 | 0 | 0.708044 | 18.1913 | 7.8 | 15.6 | -34.13 | 277 | 0 | 0.707114 | 13.1536 | | | 226.29 |
| 208 | 0 | 0.708042 | 17.8911 | 8.9 | 17.8 | -10.83 | 278 | 0 | 0.707133 | 12.4719 | | | 223.25 |
| 209 | 0 | 0.708032 | 17.5372 | 9.9 | 19.9 | -9.95 | 279 | 0 | 0.707131 | 12.1986 | | | 220.19 |
| 210 | 0 | 0.707971 | 17.7571 | 10.9 | 21.8 | -9.17 | 280 | 0 | 0.707127 | 12.2137 | | | 187.77 |
| 211 | 0 | 0.707782 | 18.7694 | 11.7 | 23.4 | -8.46 | 281 | 0 | 0.707131 | 12.5251 | | | 184.66 |

Table 2 (Continued)

| Age (Ma) | A10 <i>p</i> | $^{87}\text{Sr}/^{86}\text{Sr}$ | $\delta^{34}\text{S}$ | LIP volumes vs#1(10^3 km^3) | LIP volumes vs#2(10^3 km^3) | Marine genera* | Age (Ma) | A10 <i>p</i> | $^{87}\text{Sr}/^{86}\text{Sr}$ | $\delta^{34}\text{S}$ | LIP volumes vs#1(10^3 km^3) | LIP volumes vs#2(10^3 km^3) | Marine genera* |
|---------------|-----------------|---------------------------------|-----------------------|--|--|-------------------|----------|-----------------|---------------------------------|-----------------------|--|--|-------------------|
| Part-3 | | | | | | | | | | | | | |
| 282 | 0 | 0.707164 | 12.9692 | | | 181.53 | 353 | 0.00418 | 0.708139 | 21.1019 | | | -146.16 |
| 283 | 0 | 0.707227 | 13.2844 | | | 178.37 | 354 | 0.00574 | 0.708181 | 20.4954 | | | -148.73 |
| 284 | 0 | 0.707288 | 13.4259 | | | 175.19 | 355 | 0.00771 | 0.70823 | 19.8873 | | | -151.26 |
| 285 | 0 | 0.707341 | 13.4763 | | | 181.32 | 356 | 0.01016 | 0.708284 | 19.7276 | | | -153.76 |
| 286 | 0 | 0.707397 | 13.4927 | | | 178.1 | 357 | 0.01311 | 0.708329 | 19.7037 | | | -156.21 |
| 287 | 0 | 0.707476 | 13.4978 | | | 174.86 | 358 | 0.01658 | 0.708358 | 19.7005 | | | -158.62 |
| 288 | 0 | 0.707584 | 13.4989 | | | 171.6 | 359 | 0.02054 | 0.708379 | 19.7001 | | | -160.99 |
| 289 | 0 | 0.707684 | 13.1005 | | | 168.32 | 360 | 0.02494 | 0.708398 | 19.7 | | | -248.48 |
| 290 | 0 | 0.707735 | 12.6006 | | | 113.53 | 361 | 0.02966 | 0.708414 | 19.7 | | | -250.76 |
| 291 | 0 | 0.707744 | 12.5999 | | | 110.22 | 362 | 0.03457 | 0.708425 | 19.7 | | | -252.99 |
| 292 | 0 | 0.707743 | 12.5998 | | | 106.89 | 363 | 0.03947 | 0.708433 | 19.7 | | | -255.18 |
| 293 | 0 | 0.707778 | 12.5994 | | | 103.56 | 364 | 0.04416 | 0.708432 | 19.7 | | | -257.32 |
| 294 | 0 | 0.707866 | 12.5981 | | | 100.2 | 365 | 0.04841 | 0.708419 | 19.7012 | | | -300.07 |
| 295 | 0.00027 | 0.70793 | 12.5937 | | | 55.34 | 366 | 0.05199 | 0.708397 | 20.0302 | | | -302.11 |
| 296 | 0.10798 | 0.70796 | 12.5809 | | | 51.96 | 367 | 0.05471 | 0.708363 | 23.1873 | | | -304.1 |
| 297 | 0.79789 | 0.707979 | 12.554 | | | 15.57 | 368 | 0.05641 | 0.708298 | 23.2996 | | | -306.05 |
| 298 | 0.10798 | 0.708005 | 12.5242 | | | 12.18 | 369 | 0.05699 | 0.708214 | 23.3 | | | -307.94 |
| 299 | 0.00027 | 0.708044 | 12.5064 | | | 59.77 | 370 | 0.05641 | 0.708163 | 23.3 | | | -332.45 |
| 300 | 0 | 0.708093 | 12.4855 | | | 56.36 | 371 | 0.05471 | 0.708143 | 23.3 | | | -334.23 |
| 301 | 0 | 0.708143 | 12.3462 | | | 52.93 | 372 | 0.05199 | 0.708133 | 23.3001 | | | -335.96 |
| 302 | 0 | 0.708185 | 11.8957 | | | 49.51 | 373 | 0.04841 | 0.708126 | 23.3002 | | | -337.64 |
| 303 | 0 | 0.708214 | 11.6556 | | | 46.07 | 374 | 0.04416 | 0.708121 | 23.301 | | | -339.26 |
| 304 | 0 | 0.708236 | 11.6151 | | | 55.13 | 375 | 0.03947 | 0.70812 | 23.3041 | | | -228.49 |
| 305 | 0 | 0.708256 | 11.7365 | | | 51.69 | 376 | 0.03457 | 0.708119 | 23.3171 | | | -230 |
| 306 | 0 | 0.708269 | 12.2758 | | | 48.24 | 377 | 0.03599 | 0.708118 | 23.3709 | | | -231.45 |
| 307 | 0 | 0.708275 | 13.0445 | | | 76.8 | 378 | 0.10934 | 0.708116 | 23.5826 | | | -232.84 |
| 308 | 0 | 0.708277 | 13.4045 | | | 73.35 | 379 | 0.21297 | 0.708111 | 24.2604 | | | -168.82 |
| 309 | 0 | 0.708288 | 13.5153 | | | 69.9 | 380 | 0.26596 | 0.708104 | 25.4971 | | | -170.13 |
| 310 | 0 | 0.708286 | 13.6467 | | | 34.95 | 381 | 0.21297 | 0.70809 | 26.4337 | | | -171.33 |
| 311 | 0 | 0.708289 | 13.9179 | | | 31.5 | 382 | 0.10934 | 0.708063 | 26.7465 | | | -124.1 |
| 312 | 0 | 0.708293 | 14.3193 | | | -15.45 | 383 | 0.03599 | 0.708018 | 26.6512 | | | -125.2 |
| 313 | 0 | 0.708294 | 14.7533 | | | -18.89 | 384 | 0.0076 | 0.707967 | 25.8671 | | | -126.2 |
| 314 | 0 | 0.708291 | 15.1201 | | | -22.33 | 385 | 0.00418 | 0.707924 | 24.4323 | | | -127.2 |
| 315 | 0 | 0.708283 | 15.4076 | | | -55.26 | 386 | 0.00299 | 0.70789 | 23.6851 | | | 23 |
| 316 | 0 | 0.70827 | 15.5981 | | | -58.69 | 387 | 0.00209 | 0.707866 | 23.4217 | | | 22.1 |
| 317 | 0 | 0.708254 | 15.6284 | | | -62.11 | 388 | 0.00143 | 0.707854 | 23.1413 | | | 21.4 |
| 318 | 0 | 0.708233 | 15.4501 | | | -65.52 | 389 | 0.00096 | 0.707851 | 22.6252 | | | 99.7 |
| 319 | 0 | 0.708199 | 15.1444 | | | -75.43 | 390 | 0.00063 | 0.707852 | 21.7722 | | | 99.1 |
| 320 | 0 | 0.70816 | 14.9464 | | | -78.83 | 391 | 0.00041 | 0.707857 | 20.635 | | | 98.6 |
| 321 | 0 | 0.708123 | 14.9688 | | | -82.21 | 392 | 0.00026 | 0.707865 | 19.4038 | | | 183.1 |
| 322 | 0 | 0.708073 | 15.0476 | | | -85.59 | 393 | 0.00016 | 0.707877 | 18.2868 | | | 182.7 |
| 323 | 0 | 0.708017 | 14.9391 | | | 91.54 | 394 | 0.0001 | 0.70789 | 17.4198 | | | 182.4 |
| 324 | 0 | 0.70799 | 14.6096 | | | 88.19 | 395 | 0.00006 | 0.707899 | 16.9035 | | | 207.6 |
| 325 | 0 | 0.707987 | 14.3027 | | | 84.85 | 396 | 0.00003 | 0.707902 | 16.7243 | | | 207.5 |
| 326 | 0 | 0.707983 | 14.1447 | | | 81.53 | 397 | 0.00002 | 0.707903 | 16.6601 | | | 207.4 |
| 327 | 0 | 0.707966 | 14.0711 | | | 173.72 | 398 | 0.00001 | 0.707904 | 16.5652 | | | 235.9 |
| 328 | 0 | 0.707931 | 13.9941 | | | 170.43 | 399 | 0.00001 | 0.707908 | 16.3615 | | | 235.9 |
| 329 | 0 | 0.707879 | 13.9055 | | | 167.15 | 400 | 0 | 0.707918 | 15.9566 | | | 236 |
| 330 | 0 | 0.707823 | 13.8686 | | | 163.89 | 401 | 0 | 0.707938 | 15.3278 | | | 236.3 |
| 331 | 0 | 0.707778 | 13.9615 | | | 160.65 | 402 | 0 | 0.707978 | 14.6856 | | | 236.6 |
| 332 | 0 | 0.707752 | 14.1426 | | | 157.43 | 403 | 0 | 0.708041 | 14.499 | | | 196.4 |
| 333 | 0 | 0.707744 | 14.2528 | | | 154.23 | 404 | 0 | 0.708118 | 15.3917 | | | 196.9 |
| 334 | 0 | 0.707775 | 14.2966 | | | 151.05 | 405 | 0 | 0.708194 | 17.6014 | | | 197.4 |
| 335 | 0 | 0.707763 | 14.372 | | | 147.9 | 406 | 0 | 0.708264 | 20.1276 | | | 198 |
| 336 | 0 | 0.707776 | 14.7041 | | | 105.26 | 407 | 0 | 0.708335 | 21.8059 | | | 66.8 |
| 337 | 0 | 0.707789 | 15.4753 | | | 102.15 | 408 | 0 | 0.708422 | 22.6032 | | | 67.5 |
| 338 | 0 | 0.707806 | 16.4117 | | | 99.07 | 409 | 0 | 0.708523 | 22.9363 | | | 68.4 |
| 339 | 0.00001 | 0.707823 | 17.2977 | | | 96.01 | 410 | 0 | 0.70861 | 23.131 | | | 0.4 |
| 340 | 0.00001 | 0.707825 | 18.0314 | | | 92.98 | 411 | 0 | 0.708664 | 23.3554 | | | 1.4 |
| 341 | 0.00002 | 0.707812 | 18.5444 | | | 89.97 | 412 | 0 | 0.708693 | 23.5898 | | | -41.9 |
| 342 | 0.00003 | 0.707803 | 18.5993 | | | 86.99 | 413 | 0 | 0.708706 | 23.8394 | | | -40.7 |
| 343 | 0.00006 | 0.707812 | 18.0895 | | | 84.04 | 414 | 0 | 0.708712 | 24.1251 | | | -82.9 |
| 344 | 0.0001 | 0.707833 | 17.7435 | | | 81.13 | 415 | 0 | 0.708714 | 24.4705 | | | -81.44 |
| 345 | 0.00016 | 0.707852 | 17.6722 | | | 78.24 | 416 | 0 | 0.708715 | 24.9078 | | | -48.44 |
| 346 | 0.00026 | 0.707865 | 17.7124 | | | 3.88 | 417 | 0 | 0.708712 | 25.4545 | | | -46.84 |
| 347 | 0.00041 | 0.70788 | 17.9184 | | | 1.06 | 418 | 0 | 0.708704 | 26.0631 | | | -45.15 |
| 348 | 0.00063 | 0.707903 | 18.6073 | | | -1.73 | 419 | 0 | 0.708689 | 26.6049 | | | 32.64 |
| 349 | 0.00096 | 0.70794 | 19.8799 | | | -4.49 | 420 | 0 | 0.708666 | 26.95 | | | 34.52 |
| 350 | 0.00143 | 0.707991 | 20.8329 | | | -7.21 | 421 | 0 | 0.708633 | 27.0916 | | | 36.5 |
| 351 | 0.00209 | 0.708048 | 21.1757 | | | -9.9 | 422 | 0 | 0.708589 | 27.1488 | | | 105.58 |
| 352 | 0.00299 | 0.708098 | 21.2424 | | | -12.55 | 423 | 0 | 0.708535 | 27.2236 | | | 122.26 |

(Continued on next page)

Table 2 (Continued)

| Age (Ma) | A10 <i>p</i> | $^{87}\text{Sr}/^{86}\text{Sr}$ | $\delta^{34}\text{S}$ | LIP volumes vs#1(10^3 km^3) | LIP volumes vs#2(10^3 km^3) | Marine genera* | Age (Ma) | A10 <i>p</i> | $^{87}\text{Sr}/^{86}\text{Sr}$ | $\delta^{34}\text{S}$ | LIP volumes vs#1(10^3 km^3) | LIP volumes vs#2(10^3 km^3) | Marine genera* |
|---------------|-----------------|---------------------------------|-----------------------|--|--|-------------------|----------|-----------------|---------------------------------|-----------------------|--|--|-------------------|
| Part-4 | | | | | | | | | | | | | |
| 424 | 0 | 0.708481 | 27.3177 | | | 124.53 | 495 | 0 | 0.709111 | 32.1415 | | | -337.36 |
| 425 | 0 | 0.708436 | 27.3606 | | | 126.91 | 496 | 0 | 0.709105 | 32.1143 | | | -325.68 |
| 426 | 0 | 0.708405 | 27.2495 | | | 129.38 | 497 | 0 | 0.70909 | 32.8351 | | | -320.33 |
| 427 | 0 | 0.708382 | 26.9048 | | | 71.96 | 498 | 0 | 0.709076 | 34.12 | | | -308.32 |
| 428 | 0 | 0.708364 | 26.3579 | | | 74.64 | 499 | 0.00001 | 0.709074 | 35.5277 | | | -283.65 |
| 429 | 0 | 0.708345 | 25.7988 | | | -44.08 | 500 | 0.00005 | 0.709077 | 36.7752 | | | -271.31 |
| 430 | 0 | 0.708319 | 25.5608 | | | -41.19 | 501 | 0.00024 | 0.709081 | 37.7295 | | | -226.14 |
| 431 | 0 | 0.708284 | 26.087 | | | -38.2 | 502 | 0.00095 | 0.709082 | 38.3279 | | | -213.47 |
| 432 | 0 | 0.708242 | 27.352 | | | -35.1 | 503 | 0.00317 | 0.709083 | 38.5603 | | | -213.97 |
| 433 | 0 | 0.708204 | 28.424 | | | -31.9 | 504 | 0.00896 | 0.709083 | 38.4691 | | | -183.29 |
| 434 | 0 | 0.708175 | 28.9556 | | | -28.58 | 505 | 0.0216 | 0.709084 | 38.1337 | | | -144.12 |
| 435 | 0 | 0.708152 | 29.2316 | | | -25.16 | 506 | 0.04437 | 0.709138 | 37.6428 | | | -130.77 |
| 436 | 0 | 0.708129 | 29.4605 | | | -146.3 | 507 | 0.07767 | 0.70916 | 37.0693 | | | -128.75 |
| 437 | 0 | 0.708107 | 29.7066 | | | -142.66 | 508 | 0.11588 | 0.708943 | 36.4611 | | | -115.07 |
| 438 | 0 | 0.708084 | 29.927 | | | -138.9 | 509 | 0.14731 | 0.708804 | 35.8458 | | | -103.71 |
| 439 | 0 | 0.708057 | 29.9406 | | | -209.7 | 510 | 0.15958 | 0.70879 | 35.2407 | | | -89.67 |
| 440 | 0 | 0.70802 | 29.4217 | | | -205.72 | 511 | 0.14731 | 0.708774 | 34.6588 | | | -75.46 |
| 441 | 0 | 0.707986 | 28.1398 | | | -201.63 | 512 | 0.11588 | 0.708758 | 34.1107 | | | -61.08 |
| 442 | 0 | 0.707968 | 26.3328 | | | -197.42 | 513 | 0.07767 | 0.708739 | 33.6037 | | | -40.02 |
| 443 | 0 | 0.707961 | 24.5483 | | | -193.1 | 514 | 0.04437 | 0.70872 | 33.1456 | | | -25.28 |
| 444 | 0 | 0.707956 | 23.1576 | | | -67.66 | 515 | 0.0216 | 0.708703 | 32.7975 | | | -10.37 |
| 445 | 0 | 0.707949 | 22.2675 | | | -63.11 | 516 | 0.00896 | 0.708687 | 32.9023 | | | 2.23 |
| 446 | 0 | 0.70794 | 21.8754 | | | 264.59 | 517 | 0.00317 | 0.708673 | 33.376 | | | 17.5 |
| 447 | 0 | 0.707927 | 21.9731 | | | 269.39 | 518 | 0.00095 | 0.708658 | 33.5513 | | | 32.95 |
| 448 | 0 | 0.707914 | 22.4921 | | | 301.3 | 519 | 0.00024 | 0.708639 | 33.6085 | | | 173.09 |
| 449 | 0 | 0.707905 | 23.1411 | | | 351.63 | 520 | 0.00005 | 0.708618 | 33.6601 | | | 188.91 |
| 450 | 0 | 0.707904 | 23.6991 | | | 356.79 | | | | | | | |
| 451 | 0 | 0.70791 | 24.2087 | | | 362.07 | | | | | | | |
| 452 | 0 | 0.707926 | 24.7292 | | | 367.47 | | | | | | | |
| 453 | 0 | 0.707955 | 25.2425 | | | 408.29 | | | | | | | |
| 454 | 0 | 0.707993 | 25.6599 | | | 413.94 | | | | | | | |
| 455 | 0 | 0.708029 | 25.8326 | | | 419.72 | | | | | | | |
| 456 | 0 | 0.708057 | 25.717 | | | 425.62 | | | | | | | |
| 457 | 0 | 0.70808 | 25.4217 | | | 398.05 | | | | | | | |
| 458 | 0 | 0.708102 | 25.0586 | | | 404.21 | | | | | | | |
| 459 | 0 | 0.708129 | 24.6539 | | | 410.5 | | | | | | | |
| 460 | 0 | 0.708166 | 24.1585 | | | 416.91 | | | | | | | |
| 461 | 0 | 0.708221 | 23.4239 | | | 229.76 | | | | | | | |
| 462 | 0 | 0.708295 | 22.332 | | | 236.45 | | | | | | | |
| 463 | 0 | 0.708374 | 21.4508 | | | 121.76 | | | | | | | |
| 464 | 0 | 0.708447 | 21.5106 | | | 14.71 | | | | | | | |
| 465 | 0 | 0.708522 | 22.287 | | | 21.79 | | | | | | | |
| 466 | 0 | 0.708612 | 23.4152 | | | 29.01 | | | | | | | |
| 467 | 0 | 0.708711 | 24.6849 | | | 36.36 | | | | | | | |
| 468 | 0 | 0.708795 | 25.8873 | | | -8.15 | | | | | | | |
| 469 | 0 | 0.708843 | 26.8031 | | | -0.52 | | | | | | | |
| 470 | 0 | 0.708858 | 27.3191 | | | 7.25 | | | | | | | |
| 471 | 0 | 0.708858 | 27.5025 | | | 15.16 | | | | | | | |
| 472 | 0 | 0.708859 | 27.5302 | | | -62.29 | | | | | | | |
| 473 | 0 | 0.708865 | 27.5885 | | | -54.1 | | | | | | | |
| 474 | 0 | 0.708877 | 27.8328 | | | -45.77 | | | | | | | |
| 475 | 0 | 0.708896 | 28.3201 | | | -37.29 | | | | | | | |
| 476 | 0 | 0.708919 | 28.9359 | | | -267.67 | | | | | | | |
| 477 | 0 | 0.708939 | 29.5101 | | | -258.91 | | | | | | | |
| 478 | 0 | 0.70895 | 29.9636 | | | -249.99 | | | | | | | |
| 479 | 0 | 0.708951 | 30.2883 | | | -361.94 | | | | | | | |
| 480 | 0 | 0.70895 | 30.4858 | | | -352.73 | | | | | | | |
| 481 | 0 | 0.708956 | 30.5304 | | | -343.38 | | | | | | | |
| 482 | 0 | 0.708972 | 30.3244 | | | -333.88 | | | | | | | |
| 483 | 0 | 0.708994 | 29.7264 | | | -324.22 | | | | | | | |
| 484 | 0 | 0.709013 | 28.9989 | | | -367.92 | | | | | | | |
| 485 | 0 | 0.709029 | 28.8066 | | | -357.96 | | | | | | | |
| 486 | 0 | 0.709041 | 29.1662 | | | -347.85 | | | | | | | |
| 487 | 0 | 0.709051 | 29.7916 | | | -337.59 | | | | | | | |
| 488 | 0 | 0.709061 | 30.5368 | | | -327.17 | | | | | | | |
| 489 | 0 | 0.70907 | 31.3242 | | | -361.6 | | | | | | | |
| 490 | 0 | 0.709079 | 32.0648 | | | -350.87 | | | | | | | |
| 491 | 0 | 0.709087 | 32.6415 | | | -353.99 | | | | | | | |
| 492 | 0 | 0.709095 | 32.9378 | | | -342.95 | | | | | | | |
| 493 | 0 | 0.709102 | 32.8921 | | | -346.24 | | | | | | | |
| 494 | 0 | 0.709109 | 32.5515 | | | -334.88 | | | | | | | |

automatic localization of periodic signals, gradual shifts and abrupt interruptions, trends and onsets of trends in time-series (Riou and Vetterli, 1991). The wavelet coefficients W of a time-series $x(s)$ are calculated by a simple convolution

$$W_\psi(a, b) = \left(\frac{1}{\sqrt{a}}\right) \int x(s)\psi\left(\frac{s-b}{a}\right) ds \quad (1)$$

where ψ is the mother wavelet, a is the scale factor that determines the characteristic frequency or wavelength, and b represents the shift of the wavelet over $x(s)$ (Prokoph and Barthelmes, 1996).

The bandwidth resolution for a wavelet transform varies with

$$\Delta a = \frac{\sqrt{2}}{4\pi al} \quad (2)$$

and a location resolution

$$\Delta b = \frac{al}{\sqrt{2}} \quad (3)$$

Due to Heisenberg's uncertainty principle $\Delta a \Delta b \geq 1/4\pi$, the resolution of Δb and Δa cannot be arbitrarily small (e.g., Prokoph and Barthelmes, 1996). The parameter l is used to modify the

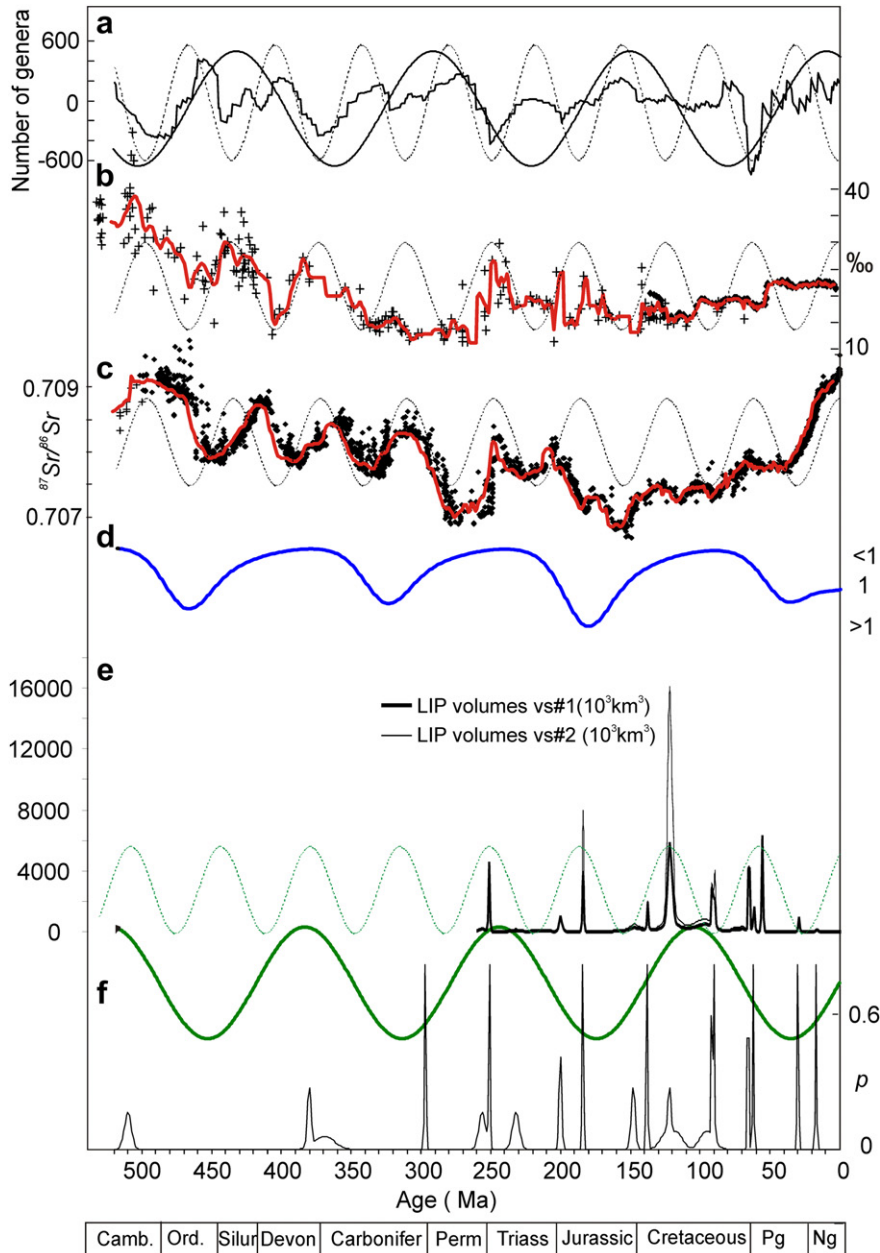


Figure 2. Geological records of last 520 Ma with best-fit 140–170 Ma and 65 Ma sine waves. a: Third order-polygonal detrended well-dated marine genera (Rhode and Muller, 2005); b: diamonds: $\delta^{34}\text{S}_{\text{barite}}$ (Paytan et al., 2004), crosses: $\delta^{34}\text{S}$ of structurally substituted sulfate (SSS) (Kampschulte and Strauss, 2004), red line: Gaussian filtered time-series; c: $^{87}\text{Sr}/^{86}\text{Sr}$ data: diamonds: low-Mg fossil shell data (Prokoph et al., 2008), crosses: whole rock samples (Shields and Veizer, 2002); d: simplified cosmic ray flux (CRF) ratio model (Shaviv and Veizer, 2003); e: LIP's volume (Ernst and Buchan, 2001; Berner, 2002) \times probability of occurrence (Prokoph et al., 2004a), note: as the total probability for each event equals 1, the total sum of $p \times$ volumes = sum all volumes; f: probability (of occurrence) of Gaussian filtered precisely dated (1% $<$ 2.5 Ma) LIP's, mostly flood and oceanic plateau basalts (Prokoph et al., 2004b), bottom: time scale (Gradstein et al., 2005).

bandwidth resolution either in favor of time or in favor of frequency. In this study, the CWT was used with the Morlet wavelet as the mother function (Morlet et al., 1982), which is expressed in its shifted and scaled version as

$$\psi_{a,b}^l(s) = \sqrt[4]{\pi} \sqrt{al} e^{-\frac{i2\pi(s-b)}{a}} e^{-\frac{1}{2}\left(\frac{s-b}{al}\right)^2} \quad (4)$$

The Morlet wavelet is a sinusoid with wavelength/scale a modulated by a Gaussian function (Torrence and Compo, 1998). Edge effects of the wavelet coefficients occur at the beginning and end of the analyzed time-series and increase with increasing wavelength (scale) and parameter l forming a ‘cone of influence of edge effects’ (Torrence and Compo, 1998). The cones of >10% influences of the edge effects are based on the wavelet-analysis parameters used and are illustrated in the scalograms. The amplitude-reducing feature of edge effects has been reduced by dividing the uncorrected amplitudes by a wavelet coefficients of control sine waves of 32 Ma, 65 Ma, and 140 Ma wavelengths for the respective wavebands.

The wavelet coefficients W are normalized by using the L1 normalization ($1/a$), replacing the commonly used $1/\sqrt{a}$, L2, or L² normalization (see Eq. (1)), which allow for an interpretation of wavelet coefficients in terms of Fourier amplitudes (e.g., Prokoph and Barthelmes, 1996). In addition, the L2 normalization of the Morlet wavelet commonly leads to overvaluing wavelet coefficients in long wavelengths compared to shorter ones, as discussed in detail by Schaeffli et al. (2007). The parameter $l = 10$ was chosen for all analyses, which provides sufficiently precise results in the resolution of time and scale (e.g., Prokoph et al., 2004b). The series of wavelengths $a_{W_{\max}}(b)$ with the strongest local wavelet coefficient $W(a, b)$ were extracted from the wavelet-coefficient matrix for waveband of 28–35 Ma, 60–70 Ma, and 130–150 Ma, because these series determine the strongest amplitude and their related wavelength in their respective waveband, independent of their absolute amplitude compared to the rest of the analyzed time-series. The wavelet-analysis technique used in this article is explained in detail in Prokoph and Barthelmes (1996). The matrix of the wavelet coefficients $W(a, b)$, the so-called ‘scalogram’, was coded in color scale (orange highest, blue lowest $W(a, b)$) for better graphical interpretation.

The cross-wavelet spectrum of two series $x(t)$ and $y(t)$ is defined by

$$W_{xy}(a, b) = W_x(a, b)W_y^*(a, b) \quad (5)$$

where $W_x(a, b)$ and $W_y(a, b)$ are the continuous wavelet transform of $x(t)$ and $y(t)$ respectively, and $*$ denotes the complex conjugate (e.g., Jury et al., 2002; Grinsted et al., 2004; Labat, 2005). The phase difference is defined by

$$\Delta\phi(b) = \tan^{-1} \frac{\int_{a_1}^{a_2} \text{Im}(W_{xy}(a, b)) da}{\int_{a_1}^{a_2} \text{Re}(W_{xy}(a, b)) da} \quad (6)$$

with b corresponding to the time lag b (Jury et al., 2002). “Im” and “Re” indicate the imaginary and real parts, respectively. The mother wavelet and parameters used in this study are the same as for the wavelet-analysis description provided above. For a detailed explanation of advantages and disadvantages of the normalization types regarding accuracy of the energy spectrum, amplitudes and white noise, as well as variance and bias of arbitrary estimated cross-wavelet spectra depending on the algorithms applied one can refer to Maraun and Kurths (2004) and Maraun et al. (2007).

4. Results

The A10-LIP occurrence record consists of over 20 discrete events with decreasing frequency toward older age (Fig. 1b). In contrast, the LIP volumes for the last 260 Ma are dominated by four roughly equally ~65 Ma spaced large volume events, independently if version 31 or #2 are considered (Fig. 1a, Tables 1 and 2). Such an ~60–65 Ma stationary cycle with minor (± 5 Ma) temporal fluctuations can be fitted to all geochemical and the detrended marine genera records (Fig. 2). In addition, a ~140 Ma cycle can be fitted to A10-LIP and marine genera record that is approximately inverse to the cosmic ray flux cycle promoted as major climate driver by Shaviv and Veizer (2003). Spectral analysis shows that all records exhibit considerable noise, but similar spectral peaks at ~140 Ma and 60–65 Ma. An ~28–35 Ma broadband spectral excursion is significant in the LIP volume data of the last 260 Ma (Fig. 3). The LIP volume record don't exhibit ~140 Ma cyclicity, but ~170 Ma cyclicity, which are essentially the same as within the uncertainties caused by the limited record length and hence limited low-frequency resolution.

Wavelet analysis highlights striking similarities in the cycle pattern between marine genera and LIP records during the last ~350 Ma, with an abrupt onset of a ~32 Ma cyclicity at ~135 Ma (Fig. 4a, b, e, f). Wavelet analysis extracted major 60–68 Ma and 140–160 Ma wavelengths for all geological records that slightly fluctuate in time (Fig. 4). Fossil and isotope record show all an increasing magnitude of the ~62 Ma cyclicity for Cambrian to Carboniferous, that is not evident in the LIP record. On average the dominant LIP cycle in the 60–80 Ma waveband is 64.5 Ma, slightly longer than the ~62 Ma cycle in fossil and geochemical records. In addition there is a ~100 Ma cyclicity for $^{87}\text{Sr}/^{86}\text{Sr}$, and for the last ~135 Ma, a ~28–35 Ma cycle for LIP probability (A10), LIP volume and marine biodiversity. The CWT parameters used implement a bandwidth uncertainty of $\sim \pm 3\%$ (see Eq. (2)). The temporal resolution is weaker (see Eq. (3)). For example a ~62 (60–65) Ma cycle detected at 300 Ma represents (to a 95% confidence level) an average wavelength for the interval of 300 ± 210 Ma (i.e. 90–510 Ma), and (to a 66% confidence level) an average for 300 ± 105 Ma.

In average, the wavelet coefficient representing cycle amplitude is significantly different for the ~32, ~62 and ~140 Ma wavelengths, except for marine genera that have about the same magnitude for all cycle lengths (Table 3). Thus, most high spectral values (Fig. 2) can be attributed to short-term fluctuations at

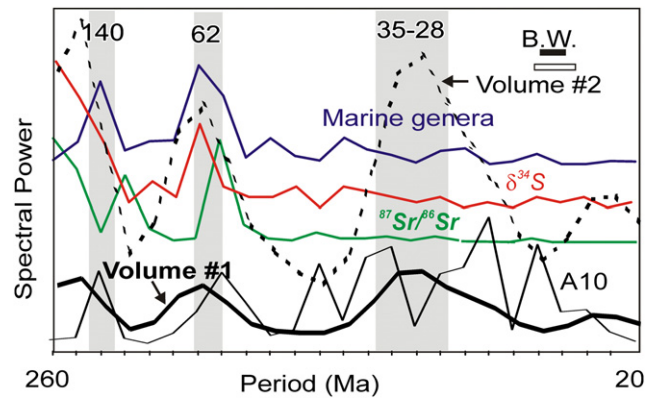


Figure 3. Spectral analysis. Spectral Power estimates for the linear detrended geological records (Fig. 2) for the last 520 Ma: vertical gray bars: bandwidth of proposed 140 Ma, ~62 Ma, and 35–28 Ma cycles, B.W. bandwidth uncertainty, note: the bandwidth for LIP volume is wider because of the shorter dataset (0–260 Ma). Lowest value for each record equals zero variance.

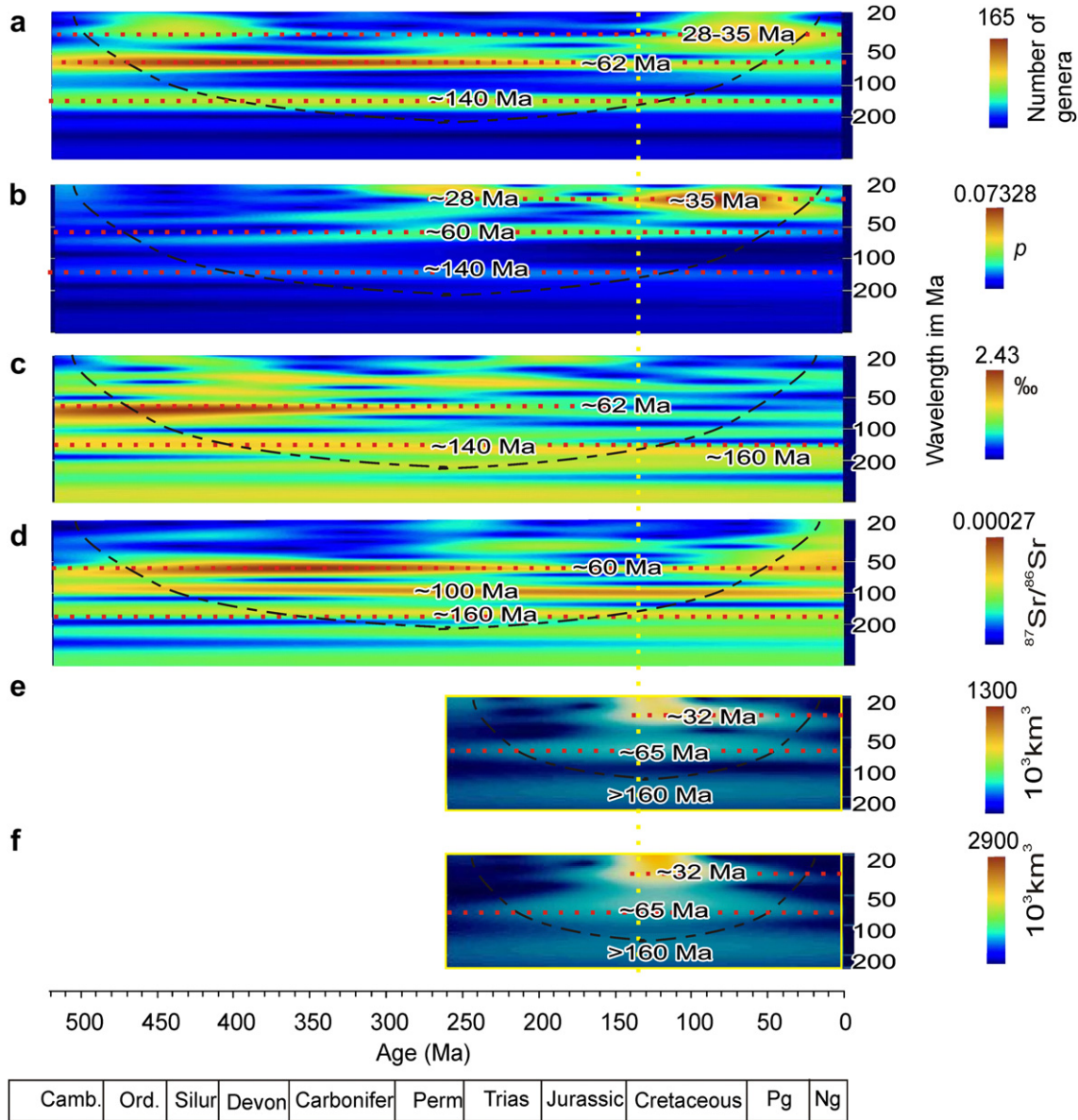


Figure 4. Wavelet analysis. a: Wavelet scalogram of detrended marine genera record; b: wavelet scalogram of marine biodiversity record; c: wavelet scalogram of probability of LIP occurrence (A10 dataset); d: wavelet scalogram of sulfur isotopes of sulfate; e: wavelet scalogram of $^{87}\text{Sr}/^{86}\text{Sr}$ record; f: LIP volumes, version #1 for last 260 Ma. Bottom: time scale (Gradstein et al., 2005). Striped curve separates frequency-time space of edge effect of <20% (above line) from >20% (below line), red dotted lines mark cycle bands, color code for wavelet amplitudes on right, vertical yellow dotted line marks the onset of ~32 Ma cyclicity in LIP and fossil records at ~135 Ma.

different wavelengths (i.e. noise), with only ~140 Ma, 62–65 Ma, and 28–35 Ma cycle bands reoccurring with at least four consecutive repetitions (Fig. 4). With the mother wavelet used and parameter $l=10$, jumps and gradual changes in the temporal pattern can only be detected in relatively short wavelengths (e.g., to

66 ± 50 Ma for a ~28 Ma-cycle). Thus, the change in the pattern at ~135 Ma has a temporal uncertainty of $\sim\pm50$ Ma at a 66% confidence level.

Before ~135 Ma, the ~65 Ma and 140 Ma LIP cyclicities are followed by a ~20 Ma delayed increase in the incorporation of heavy sulfur (^{34}S) in sulfate (Fig. 4c: phase shift 0–0.8). Fig. 5 shows that the ratios in the amplitudes of the LIP and sulfur isotope cycles are stable at ~600 km^3 LIPs' version #2 related magma production correlates with ~2‰ $\delta^{34}\text{S}_{\text{sulfate}}$ increase and an average loss of >120 well-dated marine genera. An increased LIPs' version #2 lava production is also related to a drop in $\delta^{34}\text{S}_{\text{sulfate}}$ by the same amount of ~1‰/600 $\times 10^3 \text{ km}^3$ over several million years during the last ~135 Ma (Fig. 4c, e). Thus, an extrapolation of k into the early Paleozoic (~520 Ma) suggests LIP's volume amplitudes of $\sim 1200 \times 10^3 \text{ km}^3$ at ~3‰ $\delta^{34}\text{S}_{\text{sulfate}}$ (Fig. 4d) for each 140 and 62 Ma cycle. As Fig. 2 shows, LIP, $^{87}\text{Sr}/^{86}\text{Sr}$ and $\delta^{34}\text{S}_{\text{sulfate}}$ records are

Table 3
Cycle amplitudes.

| Cycle length | 32 Ma | 65 Ma | 140 Ma |
|-----------------------|----------|------------|----------|
| Interval | 0–135 Ma | 135–260 Ma | 0–260 Ma |
| LIP vol v#1 | 498 | 316 | 276 |
| LIP vol v#2 | 931 | 666 | 584 |
| $\delta^{34}\text{S}$ | 0.79 | 0.66 | 1.78 |
| Marine genera | 124 | 127 | 123 |

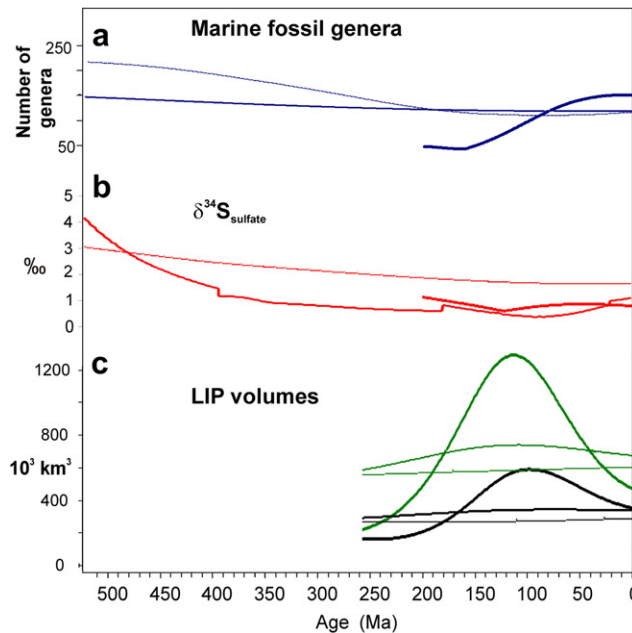


Figure 5. Edge effect corrected amplitudes (wavelet coefficients). a: marine fossil genera (blue); b: $\delta^{34}\text{S}_{\text{sulfate}}$ (red); c: LIP volumes-version #1 (black), LIP volumes-version #2 (green). Bold line: 28–35 Ma waveband, medium line: 60–70 Ma waveband, thin line: 130–150 Ma waveband. Bottom: Time scale (Gradstein et al., 2005).

well correlated, with the exception of delayed $^{87}\text{Sr}/^{86}\text{Sr}$ increase during the Silurian–Devonian. Increases of 0.001 $^{87}\text{Sr}/^{86}\text{Sr}$ correspond to $\delta^{34}\text{S}_{\text{sulfate}}$ increases of 5‰–15‰, except for the last ~135 Ma when the isotope fluctuations are uncoupled (Fig. 4). Based on the wavebands and amplitude extract by CWT (Figs. 4 and 5), with the assumption that the original LIP volume record in the Paleozoic resembles the Mesozoic/Cenozoic record, the best-fit for LIP volumes (V) would be

$$V = -(350 - 770) \times 10^3 \text{ km}^3 \sin(2\pi t/170 \text{ Ma}) + (300 - 650) \times 10^3 \text{ km}^3 \sin(2\pi t/64.5 \text{ Ma} + 2.3) \quad (7)$$

for t = time in Ma. The ~32 Ma cyclicity is not considered in the reconstruction because of its occurrence only through the last ~135 Ma.

XWT of A10-LIP occurrences with marine genera records shows that almost all cross-variability is concentrated in the 28–35 Ma, 62–65 Ma, and ~140 Ma wavelengths, with a sharp switch from ~62 to ~32 Ma cyclicity at 135 Ma (Fig. 6a). Moreover all signals in these wavelengths are approximately inverted ($-\pi$) between the LIP and other records, i.e. LIP occurrence is linked to marine genera reduction (Fig. 6b). The relationships between LIP occurrences and sulfate isotope records are also concentrated in the 28–35 Ma, 62–65 Ma, and ~140 Ma wavelengths, albeit less dominantly (Fig. 6c). Phase-shifts of ~0 (Fig. 6d) indicate a positive correlation of the ~62 and ~140 Ma signals (Fig. 2), whereas the ~32 Ma cyclicity during the last ~135 Ma is inverse correlated ($-\pi$). It is likely that the high cross-wavelet coefficients between LIP and sulfate isotope records are mostly carried by the LIP variability, because strong cross-wavelet coefficients between marine genera and geochemical records are absent in the ~32 Ma waveband, whereas ~140 and ~62 Ma cycles remain dominant (Fig. 7). The color changes at the ~62 Ma wavelength in the phase parts of the scalograms (Fig. 7b, d, f) indicate that these cycles are not as well correlated between the geochemical records as between the LIP and marine genera records. The yellow color in Fig. 7d indicates

a ~+0.5 gradient phase difference between sulfur and strontium isotopes for the ~62 and ~140 Ma cycles, i.e. the $^{87}\text{Sr}/^{86}\text{Sr}$ isotope increase lags the $\delta^{34}\text{S}_{\text{sulfate}}$ increase by up to 15 Ma.

In our study, the results of XWT (Eqs. (5) and (6)) have the same uncertainties as CWT as we use the same mother wavelet and parameters for both (see Eqs. (1)–(4)). The multiplication of the individual wavelet coefficients in Eq. (5) reduces the noise level of the cross-modulus (i.e. cross-amplitude) thus highlighting wavelengths that have a high amplitude in both time-series $x(t)$ and $y(t)$. For example, the complete independent cross-amplitude spectra of A10 vs. marine genera and sulfur vs. strontium isotopes (Fig. 6) have very similar temporal extent and relative amplitudes of the ~62 Ma cycle (stronger) and ~140 Ma cycle (weaker). The uncertainty in the phase shift is also linked to the bandwidth and temporal uncertainty (Eqs. (2) and (3)). Test runs using the parameters above on simulations of phase-shifted 140 Ma-sine waves indicate that the uncertainty for a given bandwidth (e.g., 140 ± 5 Ma) is ± 0.3 gradients.

5. Discussion

To understand the relation between LIP magmatism and sulfur isotope fluctuations, we have to point out that at present volcanic sulfur contributes 0.33×10^{12} mol/yr with a $\delta^{34}\text{S}$ of ~3‰ (Paytan et al., 2004). Currently, sulfur is either deposited to ~45% as sulfide (mostly pyrite) with isotope composition of ~−5‰ to −40‰ or as sulfate with $\delta^{34}\text{S}$ of ~+10‰ to +40‰ (Paytan et al., 2004). A marine $\delta^{34}\text{S}_{\text{sulfate}}$ increase can primarily be the result of (i) lower total sulfur input into the ocean, (ii) increased bacterial sulfide (mostly pyrite) deposition in predominantly anoxic marine basins, and (iii) decreased output from weathering (Paytan et al., 2004). The $^{87}\text{Sr}/^{86}\text{Sr}$ ratio of marine carbonates reflects primarily the relation between increased oceanic crust production (resulting in low ratios) and increased continental weathering (resulting in high ratios), respectively (Prokoph et al., 2008). Because volcanism is a source and not a sink of sulfur, we interpret the coherency between LIP cyclicity and sulfur isotopes in terms of increased sulfide deposition coeval with increased continental weathering, thus a humid global climate. This process is likely combined with increased shallow water H₂S poisoning, sluggish oceanic circulation, and oceanic anoxia as it has been suggested for some mass-extinction intervals (Kump et al., 2005). Most Paleozoic extinction events are also associated with fast global sea-level rises, anoxic events and climate warming (Hallam and Wignall, 1999). Thus, we extend the H₂S poisoning hypothesis to all major $\delta^{34}\text{S}_{\text{sulfate}}$ increases before 200 Ma, and an average marine genera biodiversity loss of ~20 marine genera/+1Δ‰ $\delta^{34}\text{S}_{\text{sulfate}}$.

During the Jurassic the linkage between LIP-related increased sulfide deposition, weathering and coeval biodiversity weakened. In general the $\delta^{34}\text{S}_{\text{sulfate}}$ dropped during the Mid-Cretaceous super plume and associated LIP eruptions (Paytan et al., 2004). Possible causes are (i) the total sulfur flux into the ocean has increased by up to 50%, (ii) the sulfate/sulfide fractionation factor decreased globally, (iii) the pyrite deposition rate decreased or (iv) a combination of the three factors (Paytan et al., 2004). Across the Cenomanian–Turonian oceanic anoxic event $\sim (0.12–0.36) \times 10^3$ Gt sulfur were removed by pyrite burial leading to a +Δ‰ $\delta^{34}\text{S}_{\text{sulfate}}$ (Ohkouchi et al., 1999; Turgeon and Creaser, 2008). The CO₂ emissions during the Mid-Cretaceous mantle plume are estimated to account for a 2.8–7.7 °C increase and could have contributed to the long-lasting Mid-Cretaceous warm period (Caldeira and Rampino, 1991). Nevertheless, the oceanic anoxic events during the Mid-Cretaceous super plume were relatively short lived with total of <3 Ma (Leckie et al., 2002) compared to the longevity of Paleozoic oceanic anoxia.

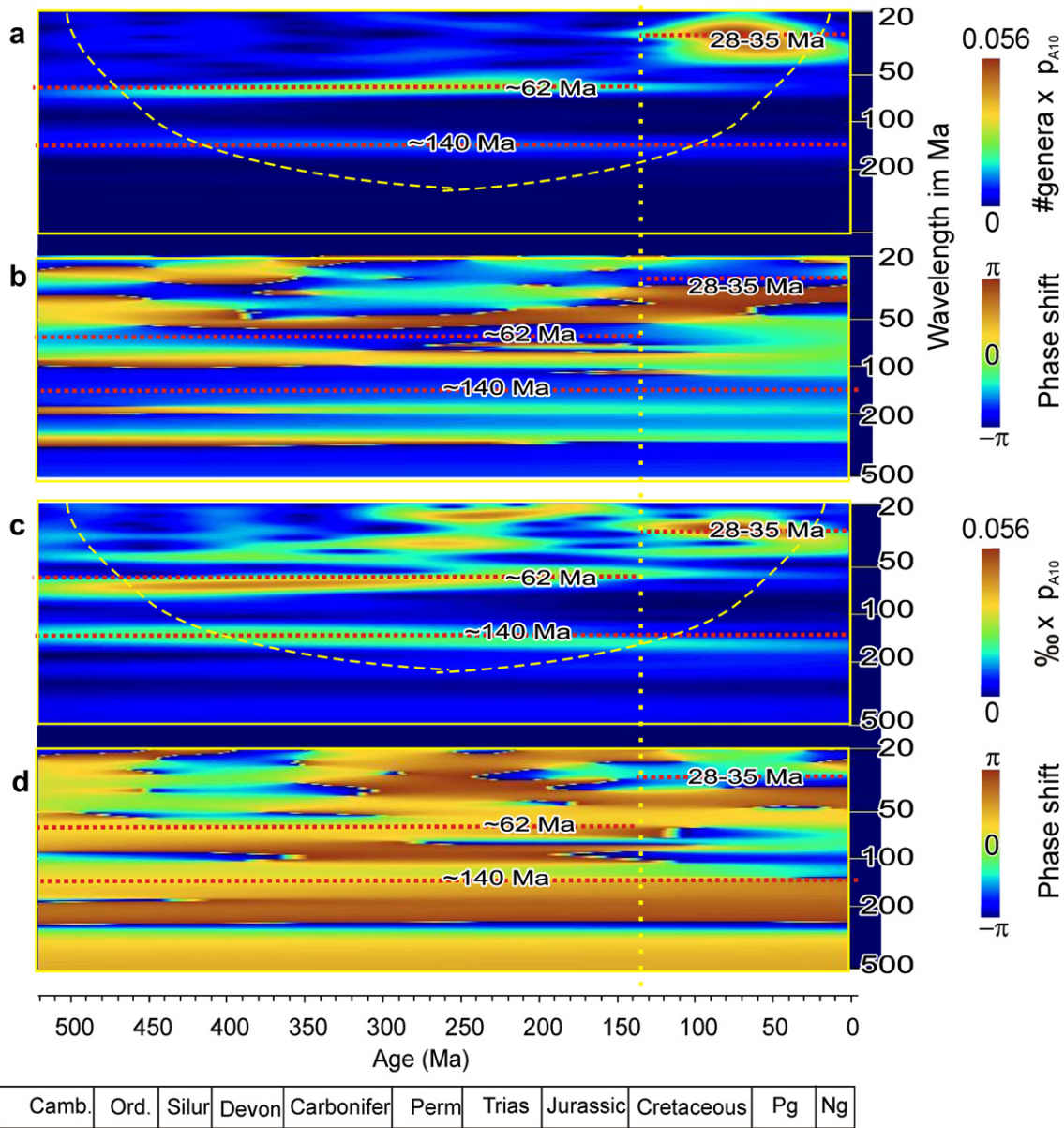


Figure 6. Cross-wavelet analysis of LIP occurrences. a: Cross-wavelet scalogram of $LIP_{A10} \times \#$ marine genera (Fig. 2a, f); b: phase-shifts between frequencies of LIP_{A10} and $\#$ marine genera (Fig. 2a, f); c: cross-wavelet scalogram of $LIP_{A10} \times \delta^{34}\text{S}_{\text{sulfate}}$ (Fig. 2b, f); d: phase-shifts between frequencies of LIP_{A10} and $\delta^{34}\text{S}_{\text{sulfate}}$ (Fig. 2b, f). Striped curves separates frequency–time space of edge effect (Torrence and Compo, 1998) of <20% (above line) from >20% (below line), red dotted lines mark cycle bands, vertical yellow dotted line marks the onset of ~32 Ma cyclicity in LIP and fossil records at ~135 Ma, color code for cross-wavelet coefficient = uncorrected cross-amplitude and phase-shifts on right.

We suggest that the shortness of the anoxic events and the quick recovery of the sulfur and carbon cycles in the last 135 Ma could be due to a more efficient biogeochemical cycling (Ridgwell, 2005), including organic carbon and sulfur storage in the deep-sea instead of in shelf seas. This could lead to the weakening of sulfur isotope and marine biodiversity fluctuation for the last ~135 Ma as shown in Fig. 2.

Thus, the addition of a 28–35 Ma geological cycle and a weakening of the ~62 Ma cycle during the last 135 Ma could be a new nonlinear response of the ocean-atmosphere system to the evolved biogeochemical processes, but this would not explain the coherent changes in the LIP cyclicity over the same time interval. However, the similarity between the phase and magnitude of the 28–35 Ma isotope cycles and the LIP cycles is strong (Figs. 2, 4). As alternative causes, changes at Earth's core–mantle boundary such as a thinning of the velocity boundary

("D") layer from ~19 to 12 km thickness, changes in the magma viscosity and/or temperature could change the size and periodicity of the LIP events (Courtillot and Besse, 1987; Courtillot and Olsen, 2007), and eventually trigger marine biogeochemical changes.

We speculate that this rarity of Paleozoic LIPs is at least partially a preservational phenomenon because (i) the recycling of ocean crust with a half-life of ~55 Ma (Veizer and Jansen, 1985) results in the removal of all oceanic LIP volcanic rock remnants older than ~190 Ma. This accounts for ~60% of all LIPs and ~60% of the total LIP volumes in the last 184 Ma; (ii) Phanerozoic sediments with a half-life of ~380 Ma (Veizer and Jansen, 1985) cover major parts of the continents and potentially hide LIPs related volcanic rocks and structures, and (iii) the high amplitudes of the ~62 Ma cycles $\delta^{34}\text{S}_{\text{sulfate}}$ and $^{87}\text{Sr}/^{86}\text{Sr}$ cycles suggest high amounts of volcanic sulfur and continental weathering-supporting fluid releases

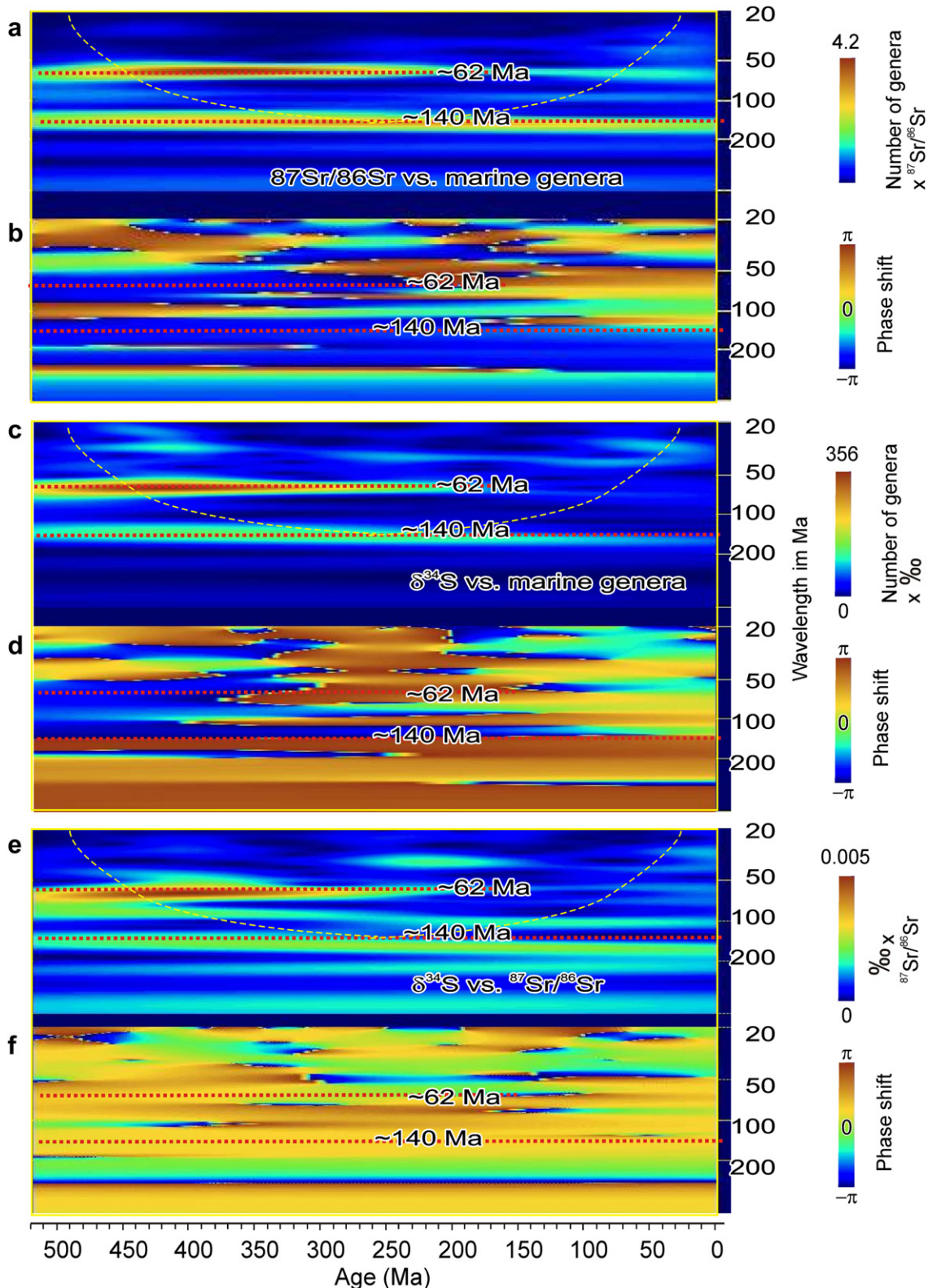


Figure 7. Cross-wavelet analysis: cross-wavelet analysis between marine genera, sulfur and strontium isotope records for the last 520 Ma: a, c, e: modulus (cross-amplitude, no edge effect correction) with color code for cross-amplitude on right side; b, d, f: phase difference with color code for phase shift in gradients on right side. Bottom: Time scale (Gradstein et al., 2005).

(Fig. 2). The LIP record improves for the Precambrian, when more of the sedimentary cover is eroded and roots of LIP's such as dyke swarms are exposed (e.g., Ernst and Buchan, 2001; Ernst and Bleeker, 2010).

LIPs are rarer in the geological record from 270 to 520 Ma and expected LIP's from a modeled ~65 Ma periodicity at ~450 Ma and ~315 Ma are missing (Fig. 2f). Some LIP's during this time interval, such as the Tarim LIP (280 Ma), are currently not included

in the data analysis due to their age uncertainty. Several studies (Young et al., 2009; Buggisch et al., 2010) hint on the possibility of a large and hitherto undetected LIP eruption triggering the Late Ordovician ice age that would explain the drop in the $^{87}\text{Sr}/^{86}\text{Sr}$ at ~ 450 Ma (Fig. 2c). The Skagerrak-centered (SC) LIP centered at ~ 300 Ma has early precursors (Torsvik et al., 2008) that may cover a predicted ~ 315 Ma LIP event. Data analysis indicates that amplitude of the 62–65 Ma LIP volume cycle is $>600 \times 10^3 \text{ km}^3$ (Eq. (7)).

The previously noted (Rampino and Stothers, 1988; Prokoph et al., 2004b) ~ 28 – 35 Ma cyclicity in geological events and paleoclimate proxies provides only insignificant total variability over the last 520 Ma, but dominates in the last ~ 200 Ma with sine wave amplitudes equivalent to the 62–65 Ma cyclicity (Fig. 4).

The 140 Ma LIP cyclicity represents the Phanerozoic part of a ~ 170 Ma (130–190 Ma) LIP cyclicity that is evident for the last 1500 Ma (Prokoph et al., 2004a). The proposed ~ 140 Ma LIP cycle is coherent with low cosmic ray flux at $>95\%$ confidence (Shaviv and Veizer, 2003) as shown in Fig. 2d as well as to the ~ 140 Ma cycle detected in the oxygen isotope record (Prokoph et al., 2008). Currently, there is no known astrophysical mechanism that can explain the ~ 140 Ma and 62 Ma sulfur and strontium isotope cyclicity. Thus, for future studies would be interesting to integrate potential galactic and terrestrial long-term driving forces on Earth ocean geochemistry, climate and biodiversity evolution.

6. Conclusion

The study reveals a periodic pattern of large igneous province (LIP) emplacement in comparison with marine isotope records, and quantifies the effects on ocean chemistry and marine biodiversity over the last 520 Ma based on compiled LIP, stable isotope and marine genera record at a data resolution of ~ 1 Ma.

Time-series analysis using wavelet and cross-wavelet transform does not only show that the ~ 140 Ma and ~ 65 Ma cycles are significant in LIP, ocean chemistry and marine biodiversity records throughout the Phanerozoic, but also highlights that a strong ~ 32 Ma cyclicity in all related records occurs simultaneously at ~ 135 Ma. The link between LIPs and biodiversity at ~ 65 Ma periodicity is particularly strong when correlating the volume of the LIPs with the marine genera record. The strong link between oceanic $\delta^{34}\text{S}_{\text{Sulfate}}$ and $^{87}\text{Sr}/^{86}\text{Sr}$ cycles and LIPs also suggest that several Paleozoic LIPs are not-yet discovered.

Acknowledgments

We thank J. Veizer for discussions, and A. Paytan for providing data. The research was funded by an NSERC discovery grant to AP.

References

- Berner, R.A., 2002. Examination of hypothesis for the Permo-Triassic boundary extinction by carbon cycle modeling. *Proceedings of the National Academy of Sciences of the United States of America* 99, 4172–4177.
- Bryan, S.E., Peate, I.U., Peate, D.W., Self, S., Jerram, D.A., Mawby, M.R., Marsh, J.S., Miller, J.A., 2010. The largest volcanic eruptions on Earth. *Earth-Science Reviews* 102, 207–229.
- Buggisch, W., Joachimski, M.M., Lehnert, O., Bergström, S.M., Repetski, J.E., Webers, G.F., 2010. Did intense volcanism trigger the first Late Ordovician icehouse? *Geology* 38, 327–330.
- Caldeira, K., Rampino, M.R., 1993. The aftermath of the K/T boundary mass extinction: biogeochemical stabilization of the carbon cycle and climate. *Paleoceanography* 8, 515–525.
- Caldeira, K., Rampino, M.R., 1991. The mid-Cretaceous superplume, carbon dioxide, and global warming. *Geophysical Research Letters* 18, 987–990.
- Coffin, M.F., Eldholm, O., 1994. Large igneous provinces: crustal structure, dimensions, and external consequences. *Review of Geophysics* 32, 1–36.
- Courtillot, V.E., Renne, P.R., 2003. On the ages of flood basalt events. *Comptes Rendus Geoscience* 335, 113–140.
- Courtillot, V., Besse, J., 1987. Magnetic field reversals, polar wander, and core-mantle coupling. *Science* 237, 1140–1147.
- Courtillot, V., Olsen, P., 2007. Mantle plumes link magnetic superchrons to phanerozoic mass depletion events. *Earth and Planetary Science Letters* 260, 495–504.
- Courtillot, V., Davaille, A., Besse, J., Stock, J., 2003. Three distinct types of hotspots in the Earth's mantle. *Earth and Planetary Science Letters* 205, 295–308.
- Ernst, R.E., Bleeker, W., 2010. Large igneous provinces (LIPs), giant dyke swarms, and mantle plumes: significance for breakup events within Canada and adjacent regions from 2.5 Ga to the present. *Canadian Journal of Earth Sciences* 47, 695–739.
- Ernst, R.E., Buchan, K.L., 2001. Large mafic magmatic events through time and links to mantle-plume heads. *Geological Society of America Special Paper* 352, 483–575.
- Gradstein, F., Ogg, J., Smith, A., 2005. *A Geologic Time Scale 2004*. Cambridge University Press, Cambridge.
- Grinsted, A., Moore, J.C., Jevrejeva, S., 2004. Application of the cross wavelet transform and wavelet coherence to geophysical time series. *Nonlinear Processes in Geophysics* 11, 561–566.
- Hallam, A., Wignall, P.B., 1999. Mass extinctions and sea-level changes. *Earth-Science Reviews* 48, 217–250.
- Isozaki, Y., 2009. Integrated “plume winter” scenario for the double-phased extinction during the Paleozoic–Mesozoic transition: the G-LB and P-TB events from a Panthalassan perspective. *Journal of Asian Earth Sciences* 36, 459–480.
- Jury, M.R., Enfield, D.B., Mélié, J., 2002. Tropical monsoons around Africa: stability of El Niño–Southern Oscillation associations and links with continental climate. *Journal of Geophysical Research* 107 (C10), 3151–3167.
- Kampschulte, A., Strauss, H., 2004. The sulfur isotopic evolution of Phanerozoic seawater based on the analysis of structurally substituted sulfate in carbonates. *Chemical Geology* 204, 255–286.
- Kuiper, K.F., Deino, A., Hilgen, F.J., Krijgsman, W., Renne, P.R., Wijbrans, J.R., 2008. Synchronizing rock clocks of Earth history. *Science* 320, 500–504.
- Kump, L.R., Pavlov, A., Arthur, M.A., 2005. Massive release of hydrogen sulfide to the ocean and atmosphere during intervals of oceanic anoxia. *Geology* 33, 397–400.
- Labat, D., 2005. Recent advances in wavelet analyses: part 1. A review of concepts. *Journal of Hydrology* 314, 275–288.
- Leckie, R.M., Bralower, T.J., Cashman, R., 2002. Oceanic anoxic events and plankton evolution: biotic response to tectonic forcing during the mid-Cretaceous. *Paleoceanography* 17, 1301–1329.
- Maraun, D., Kurths, J., 2004. Cross wavelet analysis: significance testing and pitfalls. *Nonlinear Processes in Geophysics* 11, 505–514.
- Maraun, D., Kurths, J., Holschneider, M., 2007. Nonstationary Gaussian processes in wavelet domain: synthesis, estimation, and significance testing. *Physical Review E* 75, 016707-1–016707-13.
- Melott, A.L., Bambach, R.K., Petersen, K.D., McArthur, J.M., 2012. An ~ 60 -million-year periodicity is common to marine $^{87}\text{Sr}/^{86}\text{Sr}$, fossil biodiversity, and large-scale sedimentation: what does the periodicity reflect? *The Journal of Geology* 120, 217–226.
- Morlet, J., Arehs, G., Fourgeau, I., Giard, D., 1982. Wave propagation and sampling theory. *Geophysics* 47, 203–206.
- Ohkouchi, N., Kawamura, K., Kajiwara, Y., Wada, E., Okada, M., Kanamatsu, T., Taira, A., 1999. Sulfur isotope records around Livello Bonarelli (northern Apennines, Italy) black shale at the Cenomanian–Turonian boundary. *Geology* 27, 535–538.
- Paytan, A., Kastner, M., Campbell, D., Thiemens, M.H., 2004. Seawater sulfur isotope fluctuations in the Cretaceous. *Science* 304, 1663–1665.
- Prokoph, A., Barthelmes, F., 1996. Detection of nonstationarities in geological time series: wavelet transform of chaotic and cyclic sequences. *Computer & Geoscience* 22, 1097–1108.
- Prokoph, A., Ernst, R.E., Buchan, K.L., 2004a. Time-series analysis of large igneous provinces: 3500 Ma to present. *Journal of Geology* 112, 1–22.
- Prokoph, A., Rampino, M.R., El Bilali, H., 2004b. Periodic components in the diversity of calcareous plankton and geological events over the past 230 Myr. *Palaeogeography, Palaeoclimatology, Palaeoecology* 207, 105–125.
- Prokoph, A., Shields, G.A., Veizer, J., 2008. Compilation and time-series analysis of a marine carbonate $\delta^{18}\text{O}$, $\delta^{13}\text{C}$, $^{87}\text{Sr}/^{86}\text{Sr}$ and $\delta^{34}\text{S}$ database through Earth history. *Earth-Science Reviews* 87, 113–133.
- Rampino, M.R., Stothers, R.B., 1988. Flood basalt volcanism during the past 250 million years. *Science* 241, 663–668.
- Reichow, M.K., Pringle, M.S., Al'Mukhamedov, A.I., Allen, M.B., Andreichev, V.L., Buslov, M.M., Davies, C.E., Fedoseev, G.S., Fitton, J.G., Inger, S., Medvedev, A.Y., Mitchell, C., Puchkov, V.N., Safonova, I.Y., Scott, R.A., Saunders, A.D., 2009. The timing and extent of the eruption of the Siberian Traps large igneous province: implications for the end-Permian environmental crisis. *Earth and Planetary Science Letters* 277, 9–20.
- Rhode, R.A., Muller, R.A., 2005. Cycles in fossil diversity. *Nature* 434, 208–210.
- Ridgwell, A., 2005. A Mid Mesozoic revolution in the regulation of ocean chemistry. *Marine Geology* 217, 339–357.
- Riou, O., Vetterli, M., 1991. Wavelets and signal processing. *IEEE Special Magazine*, 14–38.
- Saunders, A., Reichow, M., 2009. The Siberian Traps and the End-Permian mass extinction: a critical review. *Chinese Science Bulletin* 54, 20–37.

- Schaefli, B., Maraun, D., Holschneider, M., 2007. What drives high flow events in the Swiss Alps? Recent developments in wavelet spectral analysis and their application to hydrology. *Advances in Water Resources* 30, 2511–2525.
- Sepkoski, J., 2002. A compendium of fossil animal genera. In: Jablonski, D., Foote, M. (Eds.), *Bulletins of American Paleontology*, vol. 363. Paleontological Research Institution, Ithaca.
- Shaviv, N., Veizer, J., 2003. Celestial driver of Phanerozoic climate. *GSA Today* 13, 4–10.
- Shields, G., Veizer, J., 2002. Precambrian marine carbonate isotope database: version 1.1. *Geochemistry, Geophysics, Geosystems* 3 (6), 12.
- Svensen, H., Planke, S., Polozov, A.G., Schmidbauer, N., Corfu, F., Podladchikov, Y.Y., Jamtveit, B., 2009. Siberian gas venting and the end-Permian environmental crisis. *Earth and Planetary Science Letters* 277, 490–500.
- Torrence, C., Compo, G.P., 1998. A practical guide to wavelet analysis. *Bulletin of the American Meteorological Society* 79, 61–78.
- Torsvik, T.H., Smethurst, M.A., Burke, K., Steinberger, B., 2008. Long term stability in deep mantle structure: evidence from the ~300 Ma Skagerrak-centered large igneous province (the SCLIP). *Earth and Planetary Science Letters* 267, 444–452.
- Turgeon, S.C., Creaser, R.A., 2008. Cretaceous oceanic anoxic event 2 triggered by a massive magmatic episode. *Nature* 454, 323–326.
- Veizer, J., Jansen, S.L., 1985. Basement and sedimentary recycling-2: time dimension to global tectonics. *The Journal of Geology* 93, 625–643.
- Wignall, P.B., 2001. Large igneous provinces and mass extinctions. *Earth and Planetary Science Letters* 193, 1–33.
- Young, S.A., Saltzman, M.R., Kenneth, A., Foland, K.A., Linder, J.S., Kump, L.R., 2009. A major drop in seawater $^{87}\text{Sr}/^{86}\text{Sr}$ during the Middle Ordovician (Dariwilian): links to volcanism and climate? *Geology* 37, 951–954.